Forecasting the climate-conflict risk in Africa along climate-related scenarios and multiple socio-economic drivers

Caterina Conigliani; Valeria Costantini; Elena Paglialunga; Andrea Tancredi[1]

A Online Appendix

A.1 The grid-based dataset

We build a strongly balanced panel database covering the entire African continent based on a grid of 2,653 cells at 1° resolution (each cell covers an area of around 110x110 km).[2] The yearly database covers the time span 1990-2050, and climate-related variables are computed on the basis of monthly statistics.

The climate variables. Raw historical climate data are monthly temperature (minimum and maximum Celsius degree) and precipitation (mm per day) taken from the African Flood and Drought Monitor (AFDM) developed by Princeton University, ICI-WaRM and UNESCOIHP at 0.25° resolution. The time span covered goes from 1970 to 2016, where the first two decades (1970-1989) are used as benchmark for computing

[1]Correspondence to: Department of Economics, Roma Tre University, Via Silvio D'Amico 77, 00145, Rome, Italy. Mail: elena.paglialunga@uniroma3.it

[2]The rationale for the 1° spatial resolution is based on three points: i) geocoded disaggregated data on gross per-capita income in the form of GCP (our main variable proxying the social vulnerability to climate risk) are computed starting from the original G-Econ dataset v4.0, which is at the 1° spatial scale; ii) robustness checks on different scales conducted by La Ferrara and Harari (2018) reveal that the 1° scale provides the best model fit when the climate-conflict nexus for the whole African continent is under investigation; iii) given the country-based SSPs projections, a finer scale deserves additional (possibly arbitrary) assumptions for the disaggregation procedure.

long-term climatic changes, while the econometric estimations are based on the period 1990-2016 (Sheffield et al., 2014).[3]

Climate projection data (near-surface air temperature and precipitation) are taken from the World Climate Research Programme's Coupled Model Intercomparison Project phase 5 (CMIP5). We rely on the information from the model ESM2M developed by the Geophysical Fluid Dynamics Laboratory of the National Oceanic and Atmospheric Administration (NOAA-GFDL). This is an Earth System Model which combines an atmospheric and oceanic circulation model with representations of land, sea ice and iceberg dynamics. It also incorporates interactive biogeochemistry, including the carbon cycle, and biogeochemical components.[4]

We consider projected climate data from 2017 up to 2050 under different scenarios about future GHG emissions, i.e., different Representative Concentration Pathways (RCPs): 2.6 (mitigation scenario), 4.5 (stabilization scenario) and 8.5 (highest GHG emissions scenario).[5]

Final climate variables are computed according to the following steps. First, historical and projected monthly data on temperature (computed as the average between minimum and maximum value) and precipitations have been associated to each 1° cell. Second, we have harmonised the two data source to remove potential structural breaks corresponding

[3]AFDM reconstructs a multidecadal terrestrial water cycle based on a land surface hydrological model merged with remote sensing and reanalysis of gridded observation dataset. Then, the real-time monitoring system (2009–present) is driven by remotely sensed precipitation and atmospheric analysis data.

[4]Climate forcing includes GHG (CO2, CH4, N2O, CFC11, CFC12, HCFC22, CFC113), SD, Oz, LU, SS, BC, MD, OC. The GFDL-ESM2M model applies the Distribution Based Scaling (DBS) approach to improve usability of regional climate model projections for hydrological climate change impact studies, resulting in bias adjusted climatic variables (Yang et al., 2010).

[5]Data for the three scenarios are available at different geographical resolution and time scale. RCP 2.6 is available at a resolution of 5°x5° with monthly data, RCP 8.5 at a resolution of 0.5°x0.5° and daily data, while RCP 4.5 is available in both formats.

to the years 2016-2017: the monthly values from 2017 to 2050 are obtained by calculating the evolution of the three RCPs (with a monthly-based percentage change over year from 2016 to 2050) and applying it to the last historical absolute value available for each month of 2016.[6] Considering the harmonised monthly temperature and precipitation at the cell level (x_{imt}) we have computed three indicators.

First, for the period 1990-2050 we compute the changes in climatic conditions with respect to a long-term trend measured as the annual mean of the difference between the variable observed for each cell i in month m of year t and the average value for the same month in all j years of the benchmark period 1970-1989 ($N = 20$):

$$dx_{it} = \frac{1}{12}\sum_{m=1}^{12}\left(x_{imt}|_{t>1989} - \frac{1}{N}\sum_{j=1}^{N} x_{imj}|_{(1970\leq j<1990)}\right) \tag{1}$$

where dx_{it} represents average temperature (in Celsius) and precipitations (in mm/day) change with respect to the benchmark. We avoid potential biases from temporary peak values by computing five-year moving averages of dx_{it}.

Second, we compute the Standardized Precipitation Evapotranspiration Index (SPEI), a synthetic measure of soil humidity accounting for relative excess or deficiency of water availability that can affect the ability to meet the demands of human activities and the environment (Hayes et al., 2011). SPEI jointly accounts for variations in precipitation and temperature, and their impact on hydrological and soil humidity conditions (Parsons et al., 2019) for different timescale. Timescales equal to or shorter than 6 months are appropriate

[6] In Figure A2a and A2b we represent the harmonised trends in temperature and precipitations as monthly average across the 2,653 cells forming our grid for the time span 1970-2050.

for evaluating the short-term effects of droughts or water excess on the agricultural sector, while timescales equal to or higher than 12 months allow to determine persistent stress conditions (Pandey and Ramasastri, 2001).[7] When $SPEI_{it} = 0$ there are no significant changes in weather conditions with respect to the normal expectation (Papaioannou, 2016). Hence, we account for non-linear patterns (U-shaped) by distinguishing between positive ($SPEIp_{it}$) and negative ($SPEIn_{it}$) indices that signal, respectively, excessive wet and dry conditions.

The agricultural channel. We build a set of indicators interacting the $SPEI$ indices with the main crops growing season of each cell, proxying the indirect mechanisms through which changes in climatic conditions impact food security and consequently social and political stability (Jones et al., 2017). This methodological approach is grounded on previous research which suggests that an important channel linking climate variability to conflicts operates through shocks to agricultural production and incomes (La Ferrara and Harari, 2018). This is particularly important in developing country, which are strongly dependent on agriculture activities, strongly affected by climate variability and with limited adaptive capacity. Since the agricultural activities follow a seasonal cycle, the exposure to climate variability is heterogeneous within year: crops are more sensitive to unfavourable conditions during the growing season, and climate anomalies recorded during those months are more likely to determine lower yields and reduced agricultural

[7]We calculate monthly values of SPEI for 1, 3, 6, 12 and 36 months using the R package SPEI by Vicente-Serrano et al. (2010). We obtain yearly data by computing the annual average of the monthly values and replacing the missing values with their minimum ones. In Figure A3a and A3b we represent the trends in SPEI12 and SPEI36 as monthly average across the 2,653 cells forming our grid for the time span 1970-2050. In Figure A4 and A5 we compare average year values at the cell level for temperature and precipitations in 2020 with values at 2050 under the three RCPs. The value for 2020 is computed on the basis of RCP 4.5 here considered as the closest to historical values.

production. Crop losses impact food security and, due to lower agricultural income and higher food prices, indirectly affect the local socio-economic conditions (henceforth, for the sake of brevity, we refer to this channel in term of *indirect impacts*). Increasing resources scarcity can contribute to political instability or stimulate people to adopt adverse livelihood strategy, creating further obstacles to peace and driving instability. The risk is that heterogeneous access to food, agricultural supply and livelihood depletion could foster grievance, resource competition and low opportunity cost to engage in violence. We thus follow the approach of Von Uexkull et al. (2016) and compute our synthetic cell/year measure as the share of growing-season months in which a drought or an excess in water has been recorded.[8] In doing so, we assume that the crops' growing season remains unchanged up to 2050, which implies that we exclude any form of adaption in our models.[9]

The socio-economic variables. We compute three variables representative of the socio-economic structure, that is acknowledged as a factor strongly influencing the vulnerability to changes in climatic conditions (Burke et al., 2015; Hsiang et al., 2011; Ide et al., 2014). First, we build the gross cell product (GCP_{it}) by harmonising at the 1° geographical scale the data provided by Kummu et al. (2018).[10] Second, we take popula-

[8]We take PRIO-GRID data on the starting and ending months of the growing season at the cell level to identify the months in each cell main crop's growth season (Gleditsch et al., 2002). Following the classification defined in McKee et al. (1993), wet and drought conditions occur when $SPEI_{imt}$ is higher than 1 or lower than -1, respectively. Combining this information, we compute two indicators measuring the share of the growing season months in which the cell experiences adverse (wet/dry) climate conditions.

[9]We are aware this is a strong assumption that could be relaxed in the future research agenda by using land-use projections on cultivars and crops changes.

[10]Kummu et al. (2018) provide 5 arc-min resolution (approximately 10 km) data for two main variables: GCP per capita (PPP) and total GCP (PPP), both expressed in constant international 2011US$. Building on this variable we compute GCP at 1° by summing all values whose coordinates fall into each cell. Data for 2016 are interpolated.

tion data from the History database of the Global Environment (HYDE3.2) provided by Goldewijk et al. (2017). Data are available for the year 1990 and for the period 2000-2015 at the spatial resolution of 5 arc-min. We follow the same procedure pursued for GCP and sum all population values in those areas belonging to the 1° cell and then interpolate the intermediate missing values. Third, taking raw values for GCP and population at the 5 arc-min resolution we compute an intra-cell income distribution Gini index which should be interpreted as representative of spatial income inequality rather than individual access to economic resources.

In order to compute cell-specific information under the five SSPs up to 2050, we take country projections on GDP (Crespo Cuaresma, 2017), population (Samir and Lutz, 2017) and Gini index (Riahi et al., 2017) from the IIASA web site. To downscale country data at the grid level we first compute the cell-specific share of national GDP and population for the historical data 1990-2016. Then we apply the evolution trend of these shares during the last decade to future country GDP and population (according to the different SSPs) in order to project the cell-specific shares up to 2050.[11] As a robustness check we compare our SSPs gridded population data with those provided by Jones and O'Neill (2016), to the best of our knowledge the only spatially-scaled information from SSPs. We collapse the 7.5 arc-min resolution data for population to our grid and compare both the average trend for the whole sample (Figure A7) and the distribution across cells by 2050 for SSP3 and SSP5 as the most distant trends (Figure A8), finding the two information sets as almost

[11]In Figure A6 we provide a general overview of the average projected values of our sample for consistency with the country-based original SSPs data. For consistency reasons, we have rescaled the single values of GCP and population for each year in order to obtain a country level value as the sum of cell-based GCP and population compatible with that provided in the SSPs database.

perfectly overlapping. The projections for the intra-cell Gini index are computed as the evolution of the country Gini from SSPs applied to the cell-specific index starting from 2016, adjusted for the lower and upper bound values in order to maintain $Gini_{it} \in [0, 1]$. Given that the linkage between socio-economic vulnerability and the probability of a community to experience an intra-state battle is reinforced when the opportunity cost of fighting is lower, following Chassang and i Miquel (2009) we model the role played by income trend (rather than the level of income) as the GCP annual growth rate.

The control variables. Selected control variables at the cell level have been introduced to account for cell-based socio-economic and geographical characteristics.

First, a key element that explains the onset and dynamics of armed conflicts is the discrimination and societal cleavages across different groups living in the same community. It is not the divergence in income distribution across individuals alone that transforms competition over scarce resources into violence, but the existence of a more general economic, political, or social division between culturally defined groups (Schleussner et al., 2016). Hence, the risk that (climate-induced) resource and economic scarcity escalates into violence is stronger if the scarcity overlays with ethnic identities. Given that in African countries ethnicity strongly shapes social identity and political preferences (Basedau and Pierskalla, 2014; Von Uexkull et al., 2016) we also account for ethnic fragmentation. This is a time-invariant variable that counts the number of distinct ethnic groups coexisting within a single cell, collapsing at the grid level data from the Geo-referenced of ethnic groups (GREG) dataset provided by Weidmann et al. (2010). In a robustness check we replace GREG data with data from Geo-referencing Ethnic Power Relations (Geo-EPR),

and results remain qualitatively unchanged (see Tables A6-A7).

Additional cell-level controls are related to location-specific geographical features and the quality of living conditions which may either increase or mitigate the risk of violence. In particular, cities in developing countries are crowded places where urban population is distributed according to income capacity, with extensive slums where access to resources, jobs, and public services is largely constrained (Buhaug and Urdal, 2013). Similarly, places located at the national borders are more likely to experience political tensions and violent events related to inter-state disputes or competition over transboundary resources as water basins (De Stefano et al., 2017; O'Loughlin et al., 2012, 2014). Hence, we include two dummy variables which assume value 1 (and 0 otherwise) if, respectively: i) within the cell is located a populated places with more than 50,000 inhabitants; ii) the cell is located at the national border. On the opposite, living conditions in desert areas are so difficult that either people rarely live there, or tend to migrate in other areas, thus reducing the risk of emerging conflicts (Bosetti et al., 2021). Similarly, high forest coverage is associated to low anthropic activities, resulting in reduced risk of violence and disorders (Corrales et al., 2019). Accordingly, we take data on land coverage from the History Database of the Global Environment (HYDE), based on the original data from the Land Cover Institute (LCI), and compute two dummy variables which assume value 1 (and 0 otherwise) if, respectively, more than 50% of the cell area is covered by desert or by forest. In a robustness check, we replace the dummy variables with the continuous information on the cell's area covered by desert and forest, and results remain qualitatively unchanged (see Tables A6-A7).

Figure A1: Comparison of conflicts with ACLED and UCDP data in Africa (1997-2020)

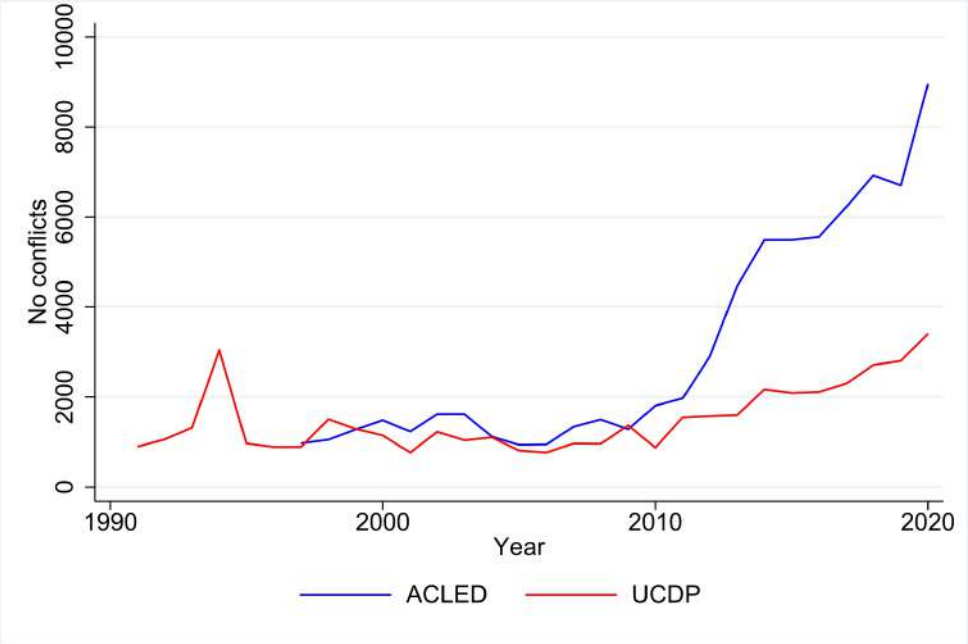

Figure A2: Trends in monthly temperature and precipitations in Africa (1970-2050)

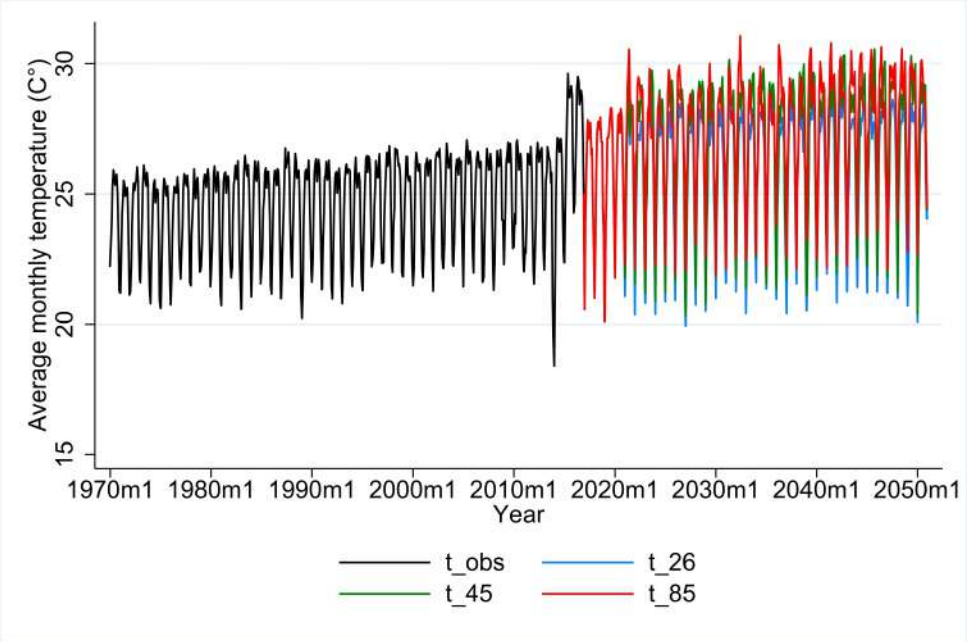

(a) Temperature

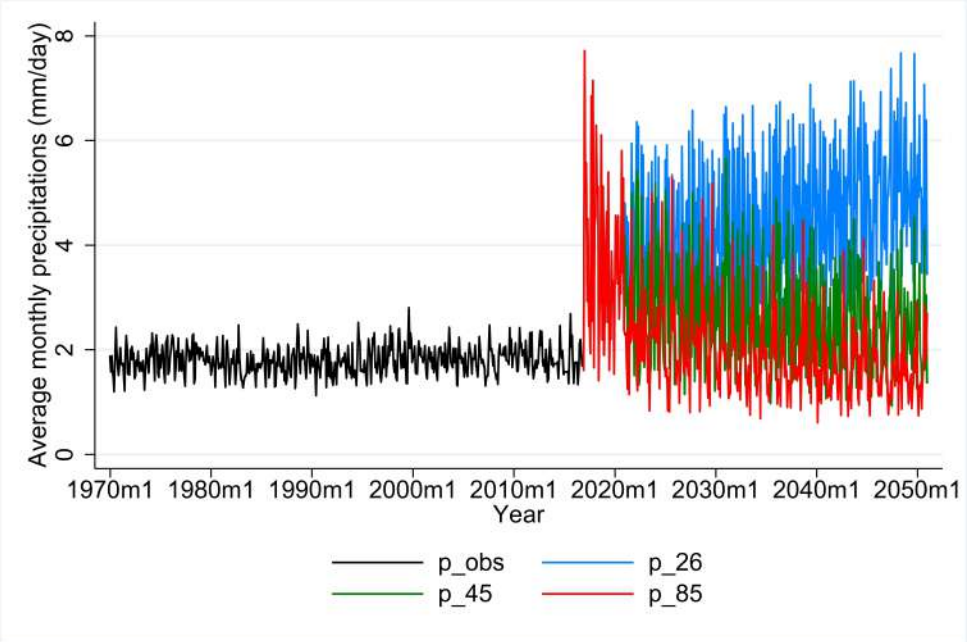

(b) Precipitations

Figure A3: Trends in monthly SPEI for Africa (1970-2050)

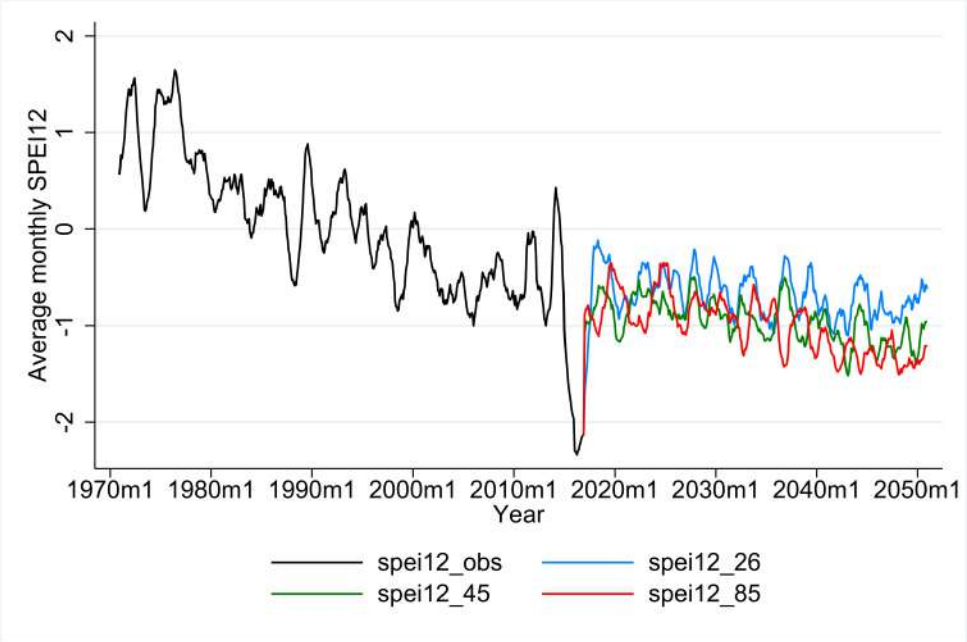

(a) SPEI12

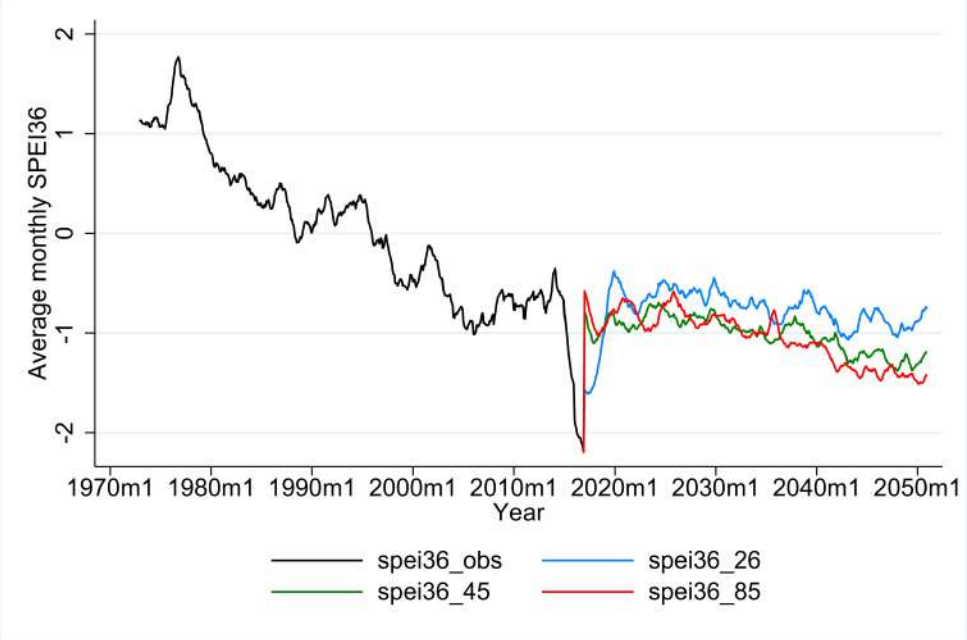

(b) SPEI36

Figure A4: Monthly-averaged yearly temperature in 2020 and 2050 (C°)

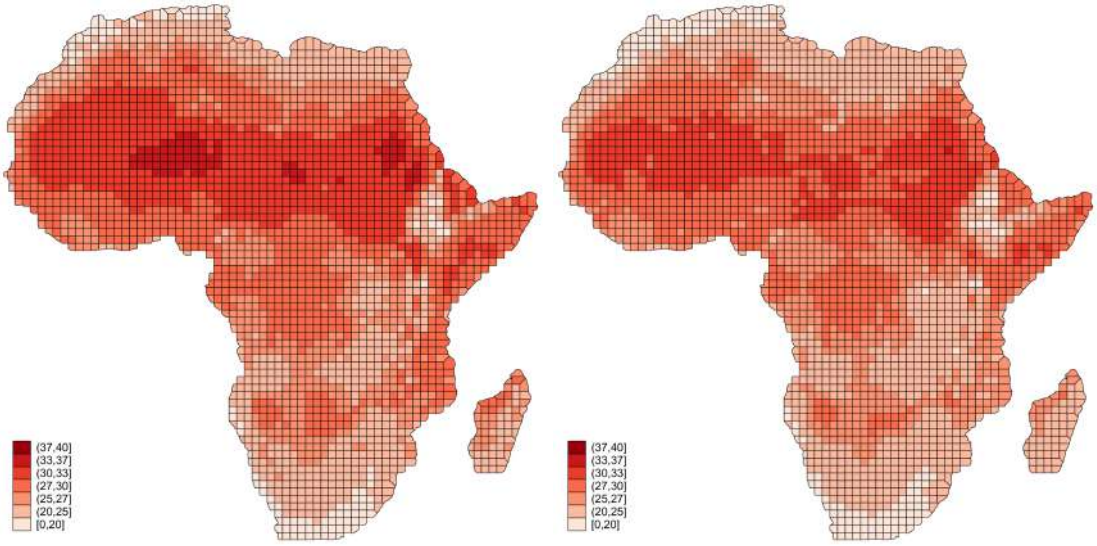

(a) 2020 - RCP 4.5

(b) 2050 - RCP 2.6

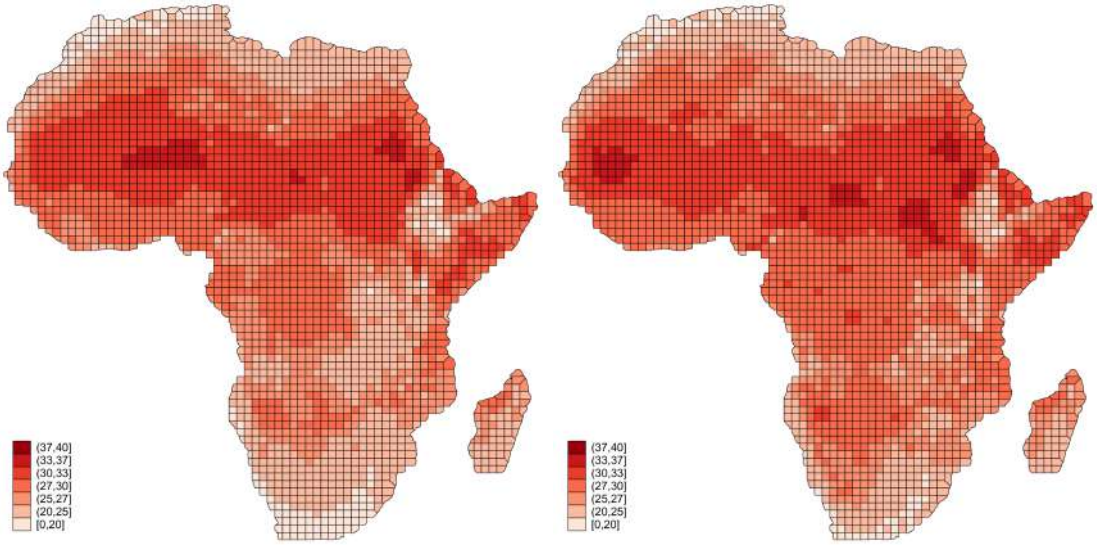

(c) 2050 - RCP 4.5

(d) 2050 - RCP 8.5

Figure A5: Monthly-averaged yearly precipitations in 2020 and 2050 (mm/day)

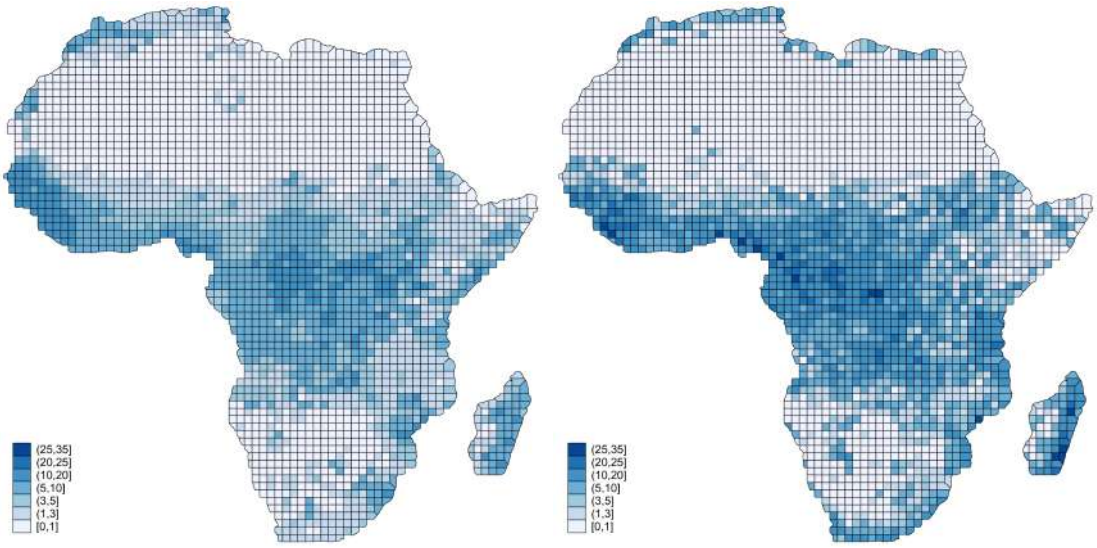

(a) 2020 - RCP 4.5

(b) 2050 - RCP 2.6

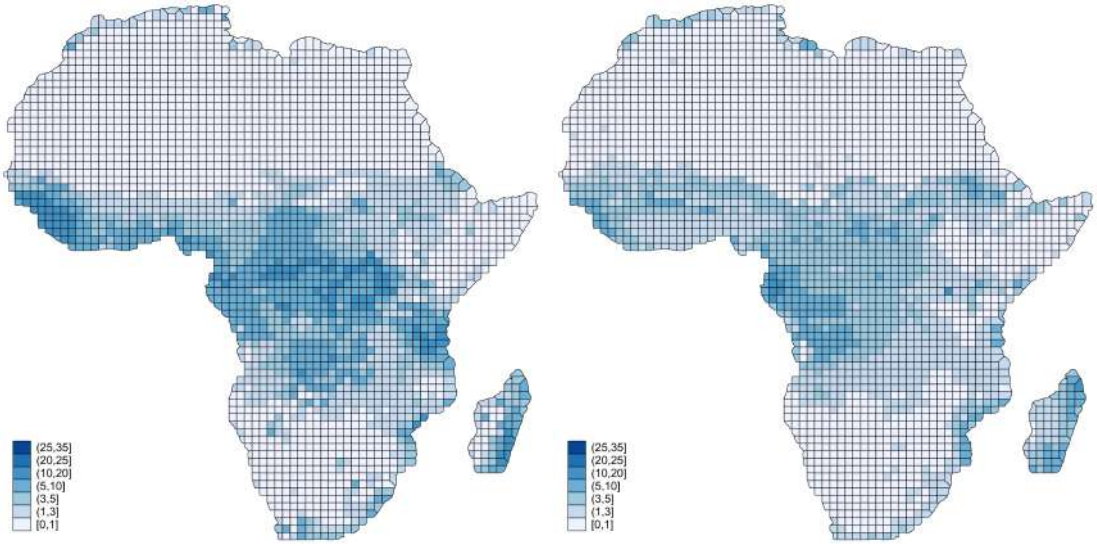

(c) 2050 - RCP 4.5

(d) 2050 - RCP 8.5

Figure A6: Average projections in main yearly variables in Africa (2020-2050)

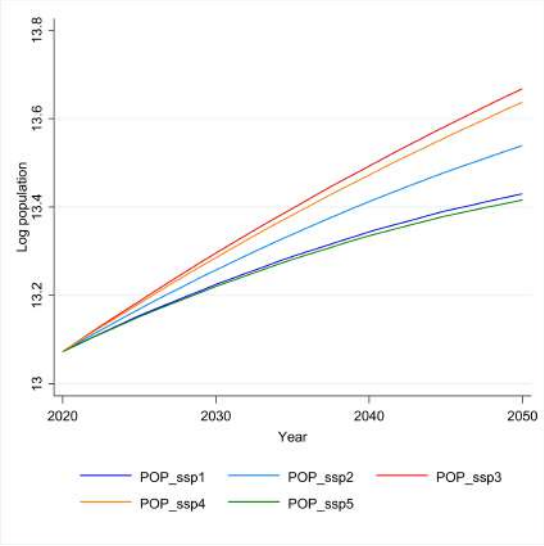

(a) Population

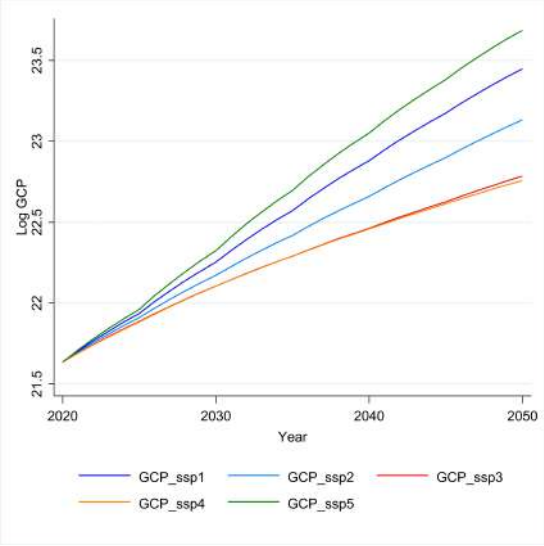

(b) Gross Cell Product (GCP)

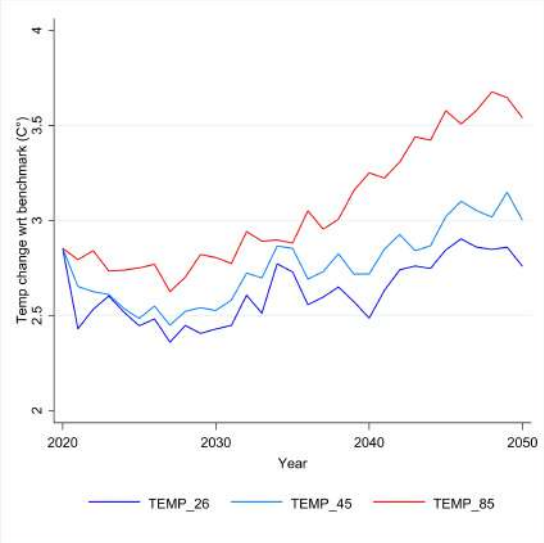

(c) Temperature change

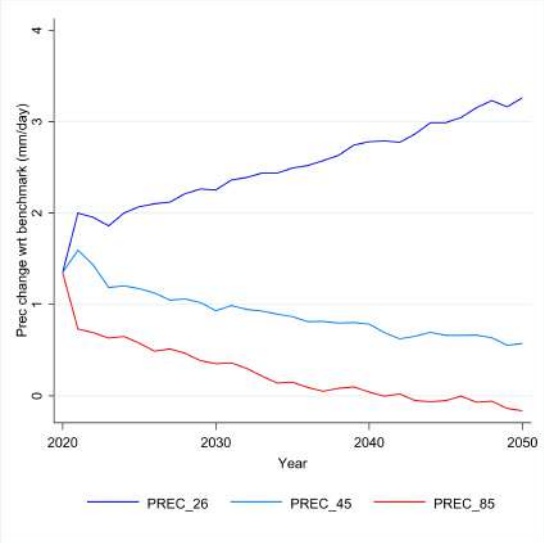

(d) Precipitation change

Figure A7: Population trend in SSPs comparing with UCAR data

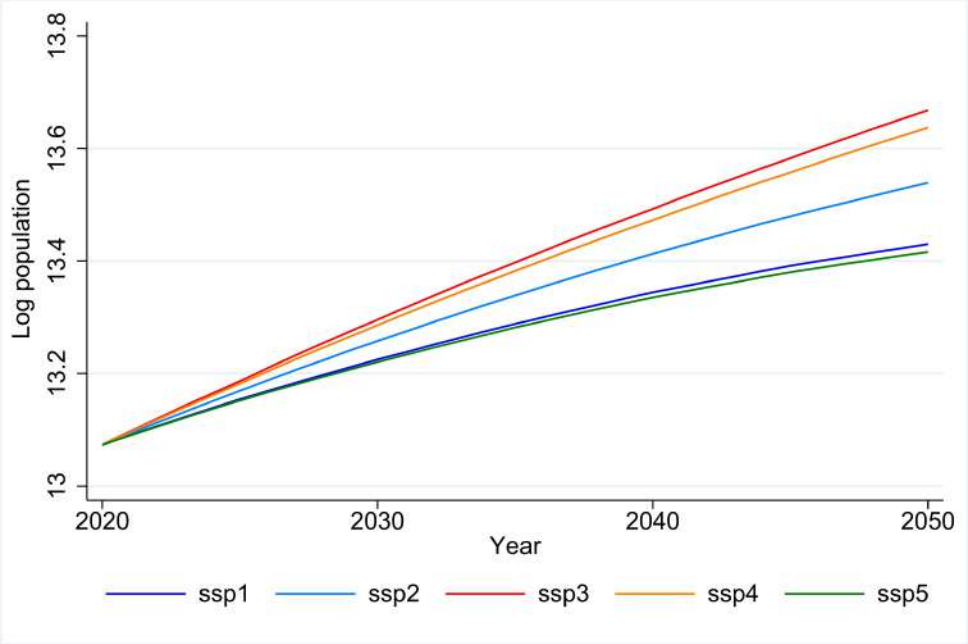

(a) Average population trends from our database

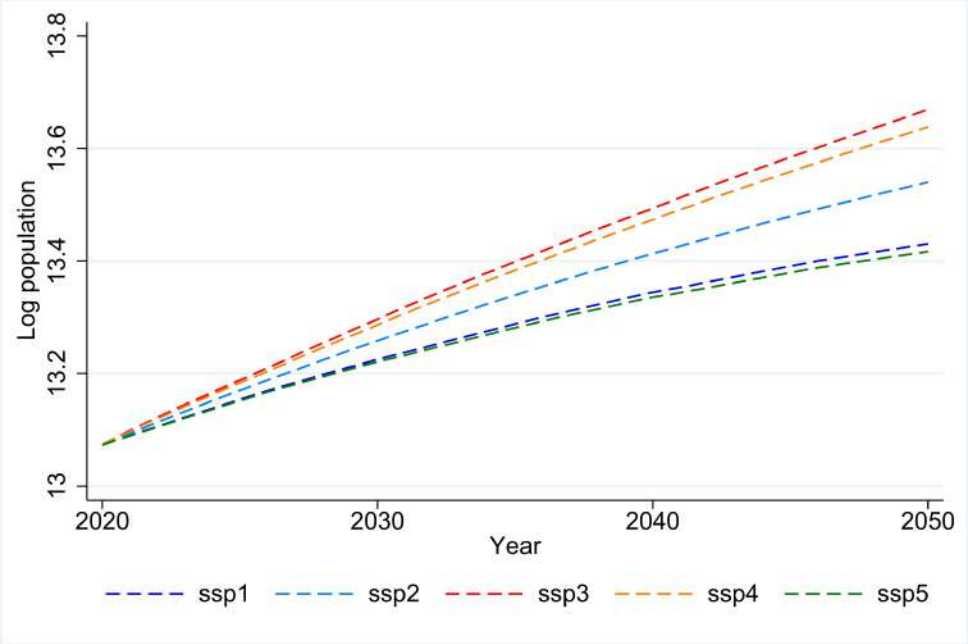

(b) Average population trends in UCAR data

Figure A8: Comparison in population distribution in 2050 with UCAR data

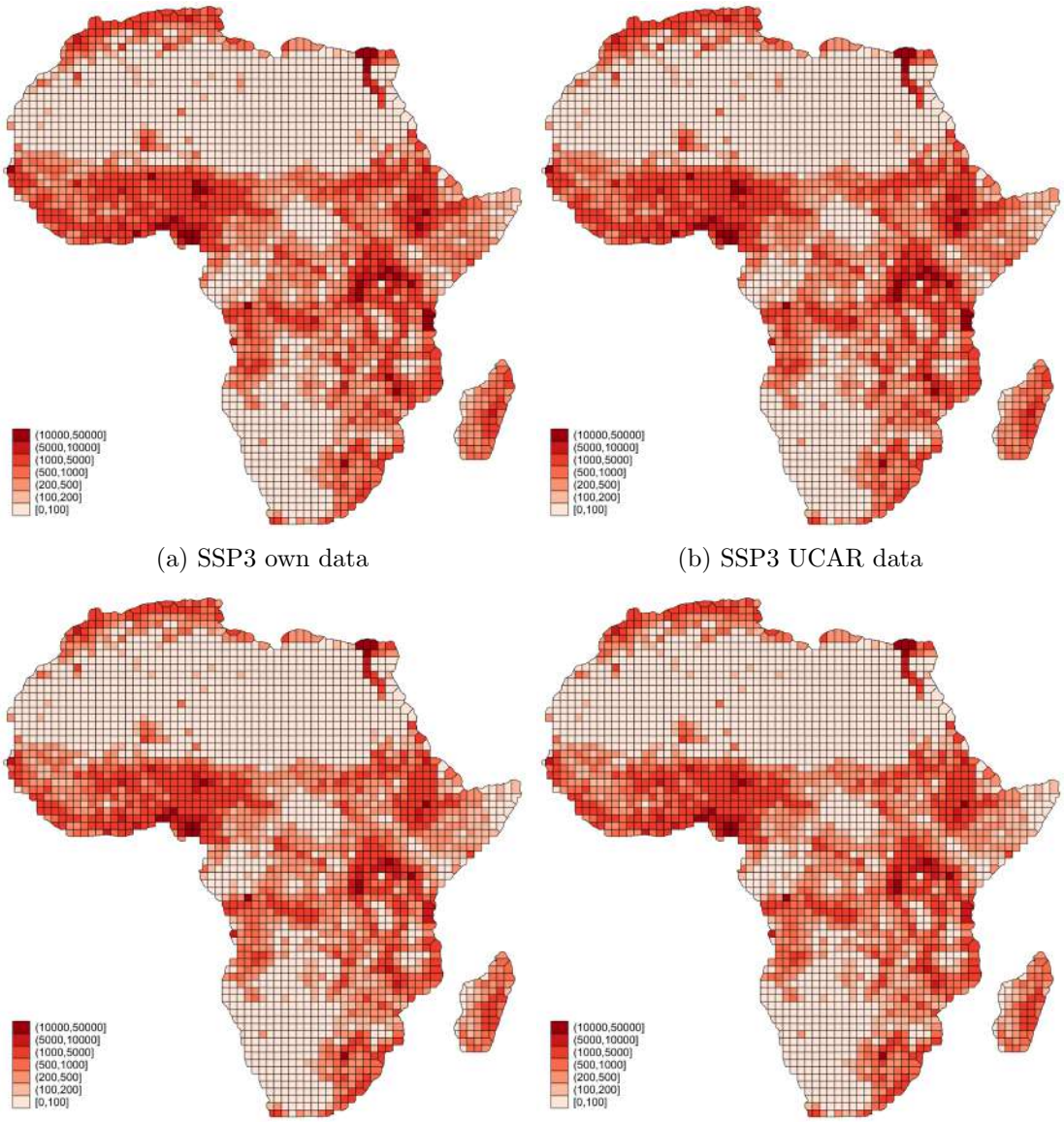

(a) SSP3 own data

(b) SSP3 UCAR data

(c) SSP5 own data

(d) SSP5 UCAR data

A.2 Econometric results

Table A1: Covariates selection on data 1990-2016 (UCDP conflicts)

	(Base)	(1)	(2)	(3)	(4)	(5)	(6)	(7)
Count model								
Population i,t-1	0.324***	0.326***	0.323***	0.324***	0.322***	0.319***	0.318***	0.314***
	(0.07)	(0.07)	(0.07)	(0.07)	(0.07)	(0.07)	(0.07)	(0.07)
Change in GCPpc i,t-1	-2.571***	-2.852***	-2.864***	-2.890***	-2.931***	-2.799***	-2.825***	-2.850***
	(0.44)	(0.48)	(0.49)	(0.50)	(0.49)	(0.45)	(0.47)	(0.47)
Gini index i,t-1	0.394	0.456	0.468	0.481	0.436	0.427	0.435	0.360
	(0.45)	(0.45)	(0.45)	(0.45)	(0.44)	(0.44)	(0.44)	(0.42)
Ethnic fract i	0.140***	0.130***	0.132***	0.133***	0.129***	0.126***	0.125***	0.125***
	(0.04)	(0.04)	(0.04)	(0.04)	(0.04)	(0.04)	(0.04)	(0.04)
Border cell (dummy) i	0.301***	0.281***	0.271***	0.261***	0.253**	0.293***	0.289***	0.286***
	(0.10)	(0.10)	(0.10)	(0.10)	(0.10)	(0.10)	(0.10)	(0.10)
Long-term temp ch i,t-1		0.218***	0.110*	0.033	0.076	0.260***	0.254***	0.284***
		(0.05)	(0.07)	(0.06)	(0.06)	(0.05)	(0.05)	(0.05)
Long-term prec ch i,t-1		0.054						
		(0.04)						
SPEI6-flo i,t-1			0.026					
			(0.09)					
SPEI6-dro i,t-1			-0.319***					
			(0.10)					
SPEI12-flo i,t-1				0.007				
				(0.08)				
SPEI12-dro i,t-1				-0.485***				
				(0.09)				
SPEI36-flo i,t-1					0.225**			
					(0.10)			
SPEI36-dro i,t-1					-0.471***			
					(0.07)			
SPEI6-flo grw i,t-1						0.541***		
						(0.17)		
SPEI6-dro grw i,t-1						0.124*		
						(0.07)		
SPEI12-flo grw i,t-1							0.531***	
							(0.15)	
SPEI12-dro grw i,t-1							0.147**	
							(0.06)	
SPEI36-flo grw i,t-1								0.708***
								(0.21)
SPEI36-dro grw i,t-1								0.056
								(0.07)
Const	-5.959***	-6.261***	-6.366***	-6.435***	-6.546***	-6.234***	-6.197***	-6.155***
	(0.87)	(0.86)	(0.86)	(0.86)	(0.85)	(0.84)	(0.84)	(0.82)
Zero model								
No conflicts it-1	-2.618***	-2.618***	-2.620***	-2.620***	-2.618***	-2.616***	-2.620***	-2.618***
	(0.10)	(0.10)	(0.10)	(0.10)	(0.10)	(0.10)	(0.10)	(0.10)
Population i,t-1	-0.180***	-0.178***	-0.177***	-0.174***	-0.177***	-0.180***	-0.181***	-0.183***
	(0.04)	(0.04)	(0.04)	(0.04)	(0.04)	(0.04)	(0.04)	(0.04)
City (dummy) i	-0.152*	-0.157*	-0.157*	-0.157*	-0.158*	-0.156*	-0.154*	-0.156*
	(0.08)	(0.08)	(0.08)	(0.08)	(0.08)	(0.08)	(0.08)	(0.08)
Desert (dummy) i	0.253**	0.279**	0.278**	0.281**	0.280**	0.262**	0.265**	0.257**
	(0.12)	(0.12)	(0.12)	(0.12)	(0.12)	(0.12)	(0.12)	(0.12)
Forest (dummy) i	0.395***	0.396***	0.401***	0.403***	0.390***	0.380***	0.380***	0.373***
	(0.13)	(0.13)	(0.13)	(0.13)	(0.13)	(0.13)	(0.13)	(0.13)
Const	4.060***	4.005***	3.998***	3.949***	3.989***	4.047***	4.053***	4.087***
	(0.52)	(0.52)	(0.52)	(0.53)	(0.52)	(0.51)	(0.51)	(0.50)
Alpha	0.852***	0.850***	0.849***	0.847***	0.841***	0.840***	0.840***	0.836***
	(0.04)	(0.04)	(0.04)	(0.04)	(0.04)	(0.04)	(0.04)	(0.04)
Observations	79590	79590	79590	79590	79590	79590	79590	79590
Log-likelihood	-31494.001	-31444.642	-31434.788	-31414.545	-31400.866	-31429.302	-31427.770	-31419.724
Chi2	8165.713	7845.509	7767.994	9711.131	7897.974	7808.418	6922.901	7240.378
AIC	63108.002	63013.284	62995.576	62955.091	62927.732	62984.603	62981.540	62965.449
BIC	63665.080	63588.932	63580.509	63540.023	63512.665	63569.536	63566.472	63550.381
Conflict No observed	46475	46475	46475	46475	46475	46475	46475	46475
Conflict No predicted	43433	44498	44104	44163	44556	44459	44500	44654

Standard errors in parentheses
* $p < 0.1$, ** $p < 0.05$, *** $p < 0.01$

Table A2: Covariates selection on data 1990-2016 (ACLED conflicts)

	(Base)	(1)	(2)	(3)	(4)	(5)	(6)	(7)
Count model								
Population i,t-1	0.474***	0.479***	0.474***	0.477***	0.473***	0.478***	0.477***	0.469***
	(0.03)	(0.03)	(0.03)	(0.03)	(0.03)	(0.03)	(0.03)	(0.03)
Change in GCPpc i,t-1	-1.344***	-1.794***	-1.790***	-1.793***	-1.761***	-1.733***	-1.729***	-1.756***
	(0.24)	(0.23)	(0.23)	(0.24)	(0.23)	(0.23)	(0.23)	(0.23)
Gini index i,t-1	0.748***	0.841***	0.869***	0.852***	0.806***	0.802***	0.822***	0.750***
	(0.28)	(0.29)	(0.29)	(0.29)	(0.28)	(0.28)	(0.29)	(0.28)
Ethnic fract i	0.158***	0.143***	0.143***	0.145***	0.143***	0.140***	0.139***	0.141***
	(0.03)	(0.03)	(0.03)	(0.03)	(0.03)	(0.03)	(0.03)	(0.03)
Border cell (dummy) i	0.473***	0.456***	0.439***	0.439***	0.438***	0.462***	0.455***	0.442***
	(0.08)	(0.08)	(0.08)	(0.08)	(0.08)	(0.08)	(0.08)	(0.08)
Long-term temp ch i,t-1		0.232***	0.228***	0.197***	0.248***	0.320***	0.327***	0.362***
		(0.03)	(0.04)	(0.04)	(0.04)	(0.03)	(0.03)	(0.03)
Long-term prec ch i,t-1		0.119***						
		(0.02)						
SPEI6-flo i,t-1			0.333***					
			(0.07)					
SPEI6-dro i,t-1			-0.268***					
			(0.08)					
SPEI12-flo i,t-1				0.296***				
				(0.06)				
SPEI12-dro i,t-1				-0.343***				
				(0.08)				
SPEI36-flo i,t-1					0.469***			
					(0.07)			
SPEI36-dro i,t-1					-0.285***			
					(0.06)			
SPEI6-flo grw i,t-1						0.788***		
						(0.12)		
SPEI6-dro grw i,t-1						0.120**		
						(0.06)		
SPEI12-flo grw i,t-1							0.812***	
							(0.09)	
SPEI12-dro grw i,t-1							0.126**	
							(0.05)	
SPEI36-flo grw i,t-1								0.953***
								(0.13)
SPEI36-dro grw i,t-1								0.014
								(0.05)
Const	-7.071***	-7.423***	-7.688***	-7.743***	-7.699***	-7.572***	-7.579***	-7.410***
	(0.48)	(0.49)	(0.49)	(0.49)	(0.47)	(0.47)	(0.48)	(0.45)
Zero model								
No conflicts it-1	-2.094***	-2.132***	-2.135***	-2.136***	-2.133***	-2.125***	-2.134***	-2.123***
	(0.09)	(0.10)	(0.10)	(0.10)	(0.10)	(0.10)	(0.10)	(0.10)
Population i,t-1	-0.263***	-0.259***	-0.261***	-0.258***	-0.260***	-0.258***	-0.258***	-0.263***
	(0.03)	(0.03)	(0.03)	(0.03)	(0.03)	(0.03)	(0.03)	(0.03)
City (dummy) i	-0.414***	-0.431***	-0.434***	-0.436***	-0.438***	-0.441***	-0.441***	-0.442***
	(0.07)	(0.07)	(0.07)	(0.07)	(0.07)	(0.07)	(0.07)	(0.07)
Desert (dummy) i	0.408***	0.470***	0.485***	0.482***	0.493***	0.459***	0.473***	0.478***
	(0.11)	(0.12)	(0.12)	(0.12)	(0.12)	(0.12)	(0.12)	(0.12)
Forest (dummy) i	0.454***	0.457***	0.454***	0.458***	0.449***	0.454***	0.454***	0.466***
	(0.12)	(0.12)	(0.12)	(0.12)	(0.12)	(0.12)	(0.12)	(0.12)
Const	4.323***	4.213***	4.221***	4.185***	4.206***	4.204***	4.195***	4.258***
	(0.36)	(0.38)	(0.38)	(0.38)	(0.38)	(0.37)	(0.38)	(0.37)
Alpha	0.722***	0.719***	0.722***	0.720***	0.717***	0.714***	0.715***	0.709***
	(0.04)	(0.04)	(0.04)	(0.04)	(0.04)	(0.04)	(0.04)	(0.04)
Observations	61019	61019	61019	61019	61019	61019	61019	61019
Log-likelihood	-41308.969	-41141.711	-41098.941	-41084.330	-41068.141	-41106.205	-41096.899	-41072.174
Chi2	1568.011	1545.468	1604.330	1583.751	1616.546	1611.662	1664.399	1793.191
AIC	82737.939	82407.422	82323.883	82294.659	82262.283	82338.410	82319.798	82270.348
BIC	83279.075	82966.597	82892.076	82862.852	82830.476	82906.604	82887.991	82838.541
Conflict No observed	73737	73737	73737	73737	73737	73737	73737	73737
Conflict No predicted	71911	74588	73302	72893	73461	73759	73971	73990

Standard errors in parentheses
* $p < 0.1$, ** $p < 0.05$, *** $p < 0.01$

Figure A9: Model comparison on mean squared Pearson residuals (UCDP and ACLED)

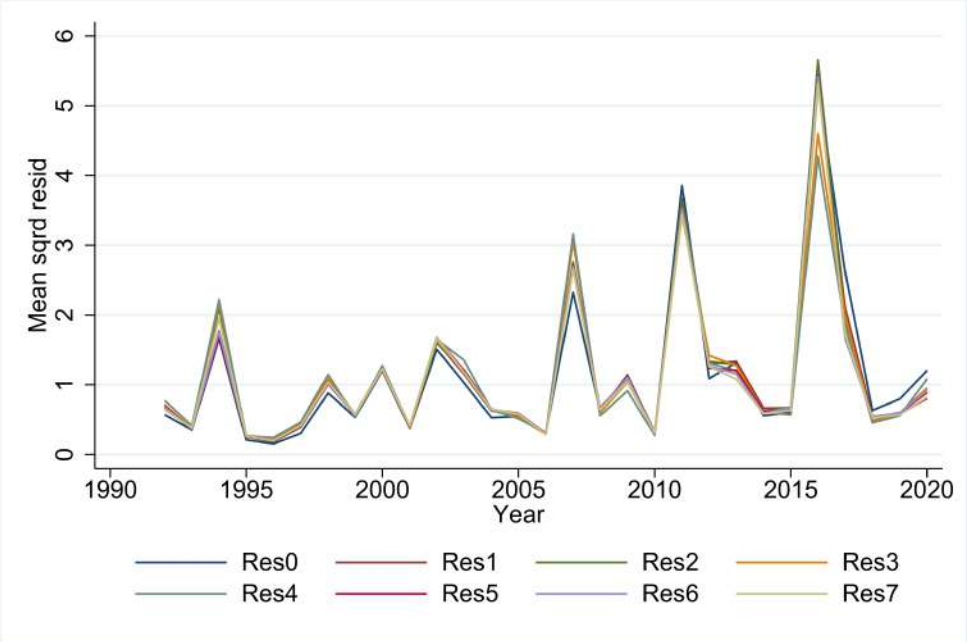

(a) UCDP (1990-2020)

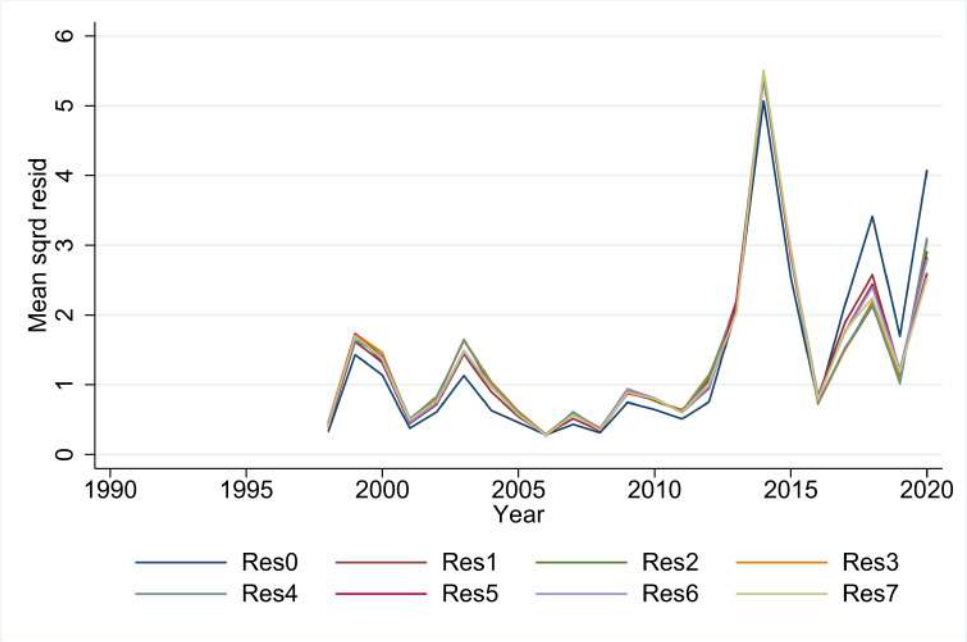

(b) ACLED (1997-2020)

Figure A10: Conflicts by cell in 2050 (UCDP)

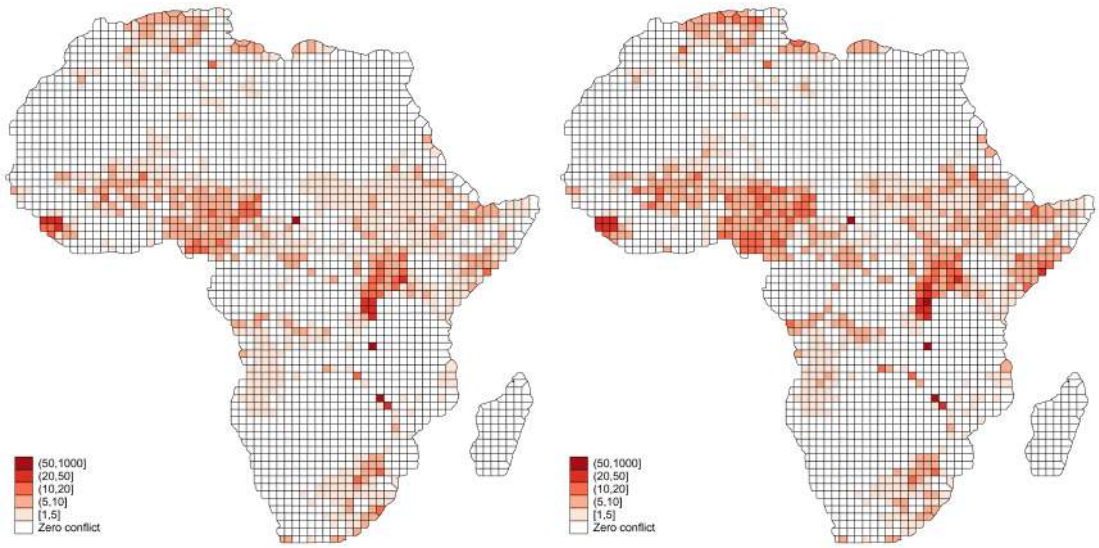

(a) SSP1

(b) SSP3

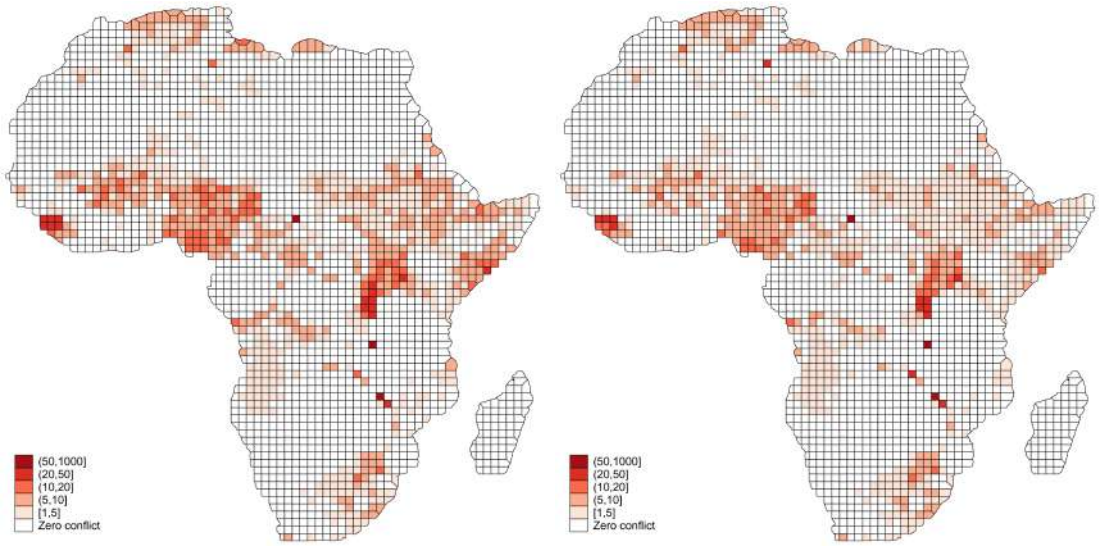

(c) SSP4

(d) SSP5

Figure A11: Conflicts by cell in 2050 (ACLED)

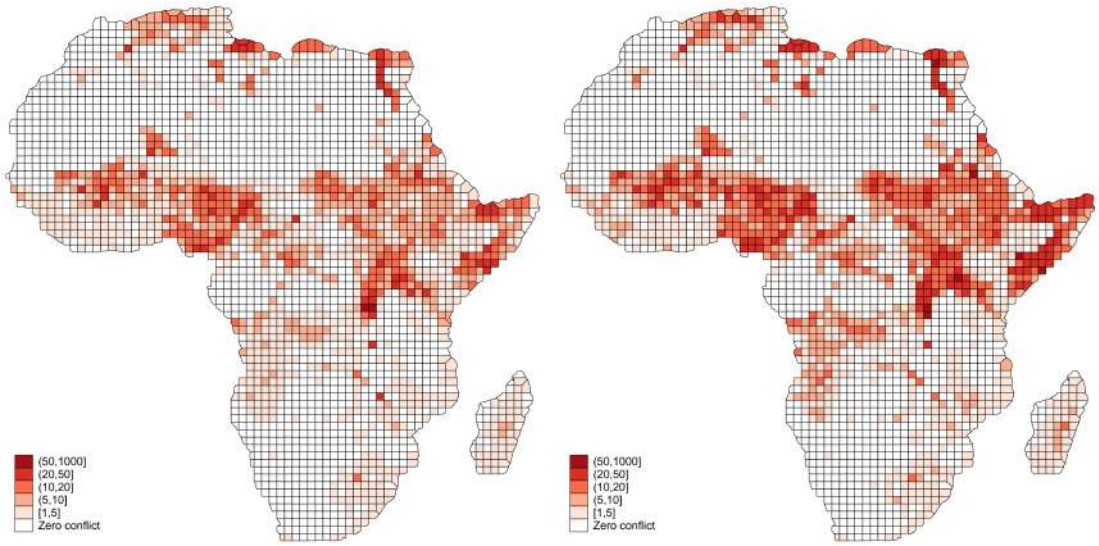

(a) SSP1 (b) SSP3

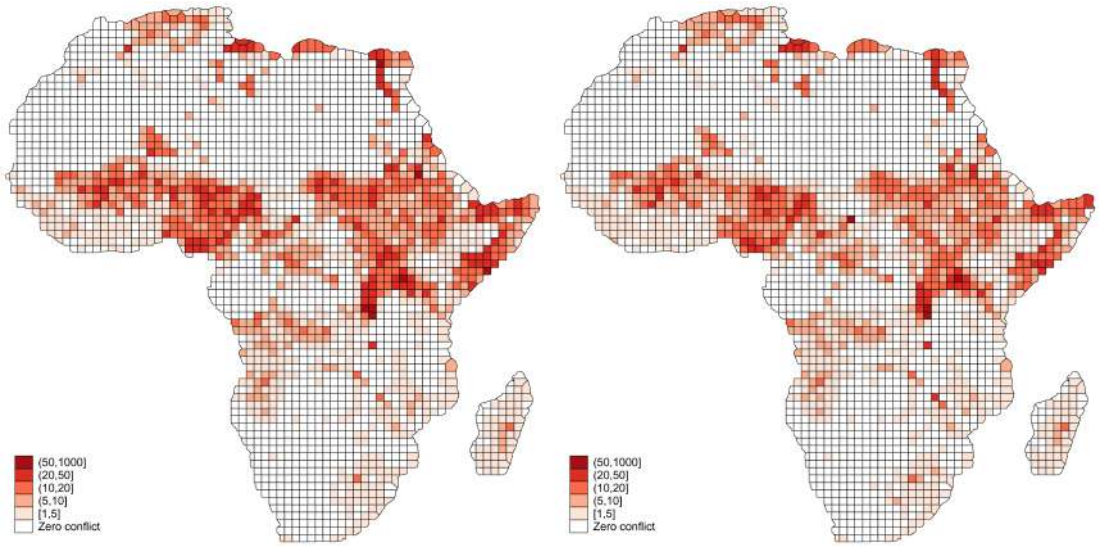

(c) SSP4 (d) SSP5

Table A3: Global Moran's I of Pearson residuals

	UCDP			ACLED		
	2018	2019	2020	2018	2019	2020
Distance weight						
W_1	0.162 ***	0.199 ***	0.237 ***	0.175 ***	0.150 ***	0.176 ***
	(16.61)	(20.56)	(26.60)	(17.90)	(16.21)	(22.61)
W_2	0.116 ***	0.135 ***	0.170 ***	0.119 ***	0.105 ***	0.126 ***
	(17.78)	(20.90)	(28.58)	(18.27)	(16.99)	(24.28)
W_3	0.090 ***	0.103 ***	0.129 ***	0.092 ***	0.081 ***	0.096 ***
	(17.77)	(20.54)	(27.98)	(18.21)	(16.82)	(23.77)
W_4	0.081 ***	0.092 ***	0.116 ***	0.082 ***	0.073 ***	0.085 ***
	(18.16)	(20.80)	(28.41)	(18.38)	(17.28)	(23.93)
W_5	0.069 ***	0.075 ***	0.094 ***	0.070 ***	0.061 ***	0.069 ***
	(18.18)	(19.88)	(27.01)	(18.45)	(17.11)	(22.85)

* $p < 0.1$, ** $p < 0.05$, *** $p < 0.01$. Z-scores reported in parentheses. Moran's I computed on Pearson residuals from econometric estimation of model 7.

Figure A12: W_d comparison on mean squared Pearson residuals (UCDP and ACLED)

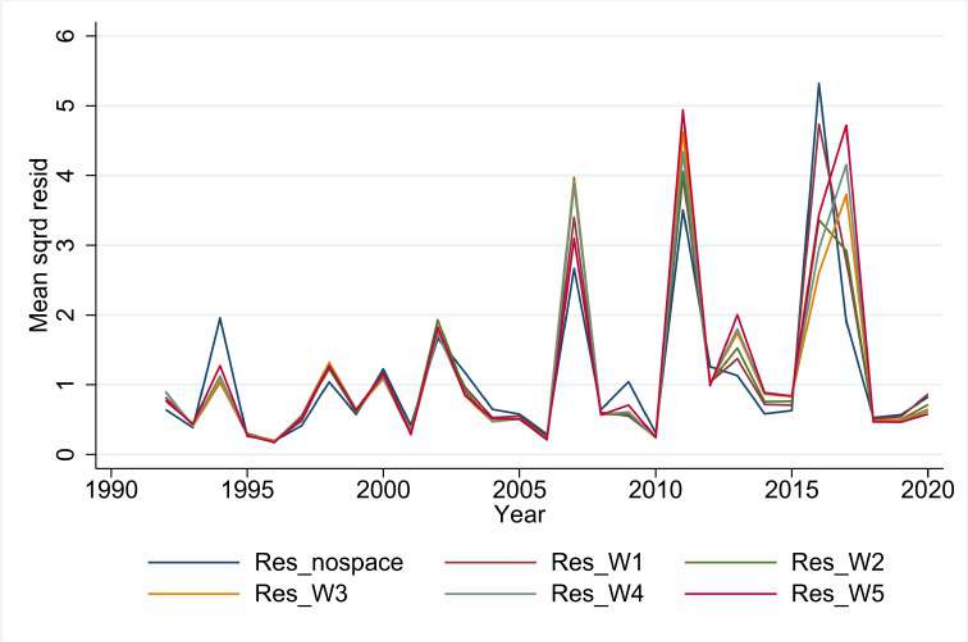

(a) 1990-2020 UCDP

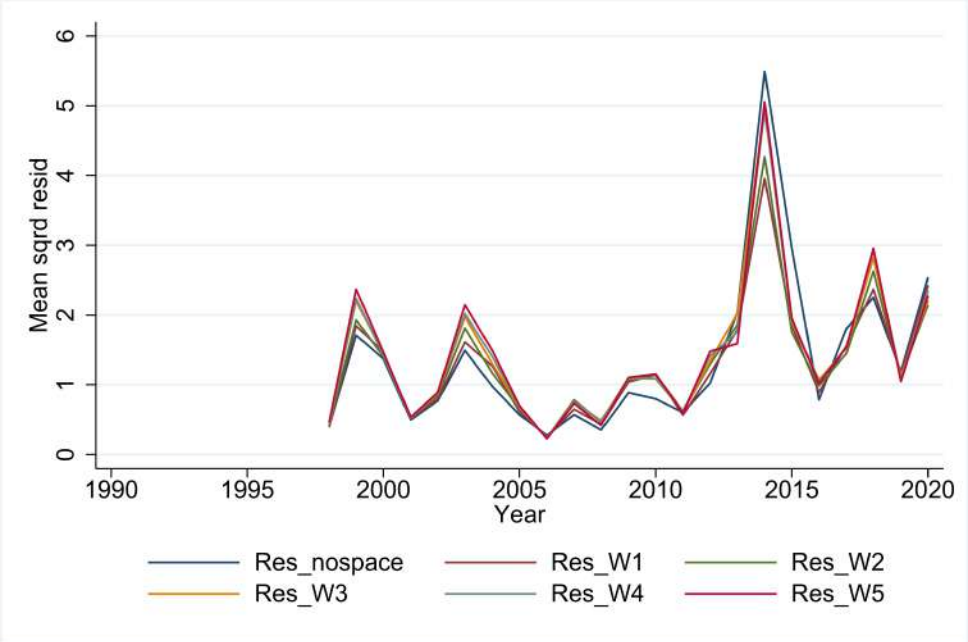

(b) 1997-2020 (ACLED)

Figure A13: Herfindal concentration index of GCP per capita ($W_d = 533$ km)

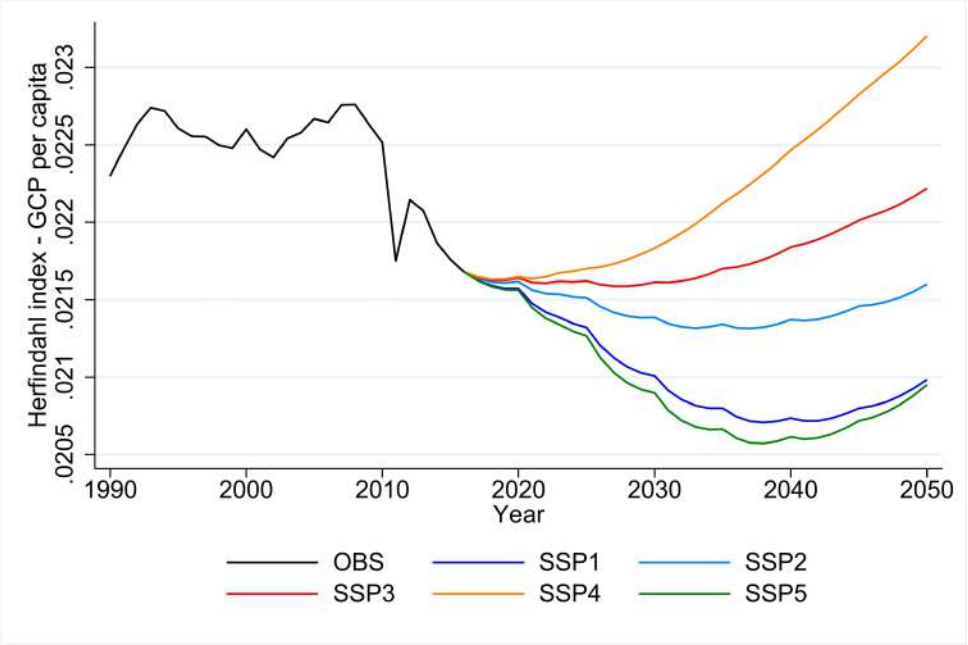

Table A4: Alternative W_d matrix with UCDP (model 7)

	W_1	W_2	W_3	W_4	W_5
Count model					
Population i,t-1	0.323***	0.316***	0.315***	0.314***	0.312***
	(0.06)	(0.05)	(0.05)	(0.06)	(0.06)
W_dPopulation it-1	-0.094*	-0.138**	-0.177***	-0.201***	-0.231***
	(0.05)	(0.06)	(0.05)	(0.05)	(0.05)
Change in GCPpc i,t-1	-5.510***	-5.362***	-5.031***	-4.744***	-4.407***
	(1.36)	(1.23)	(1.16)	(1.13)	(1.07)
W_dChange in GCPpc it-1	3.299**	3.322**	3.117**	2.853**	2.643*
	(1.48)	(1.38)	(1.37)	(1.37)	(1.38)
Gini index i,t-1	0.303	0.298	0.319	0.259	0.207
	(0.40)	(0.38)	(0.37)	(0.38)	(0.37)
W_dGini index it-1	-2.100***	-3.382***	-4.759***	-5.158***	-5.915***
	(0.62)	(0.71)	(0.80)	(0.89)	(0.98)
Ethnic fract i	0.118***	0.112***	0.109***	0.109***	0.111***
	(0.04)	(0.04)	(0.04)	(0.04)	(0.04)
Border cell (dummy) i	0.279***	0.275***	0.273***	0.270***	0.266***
	(0.10)	(0.10)	(0.10)	(0.09)	(0.09)
Long-term temp ch i,t-1	0.054	0.039	0.001	-0.001	-0.023
	(0.11)	(0.11)	(0.10)	(0.10)	(0.10)
W_dLong-term temp ch it-1	0.296**	0.335***	0.393***	0.400***	0.426***
	(0.13)	(0.13)	(0.12)	(0.12)	(0.12)
SPEI36-flo grw i,t-1	0.584**	0.509**	0.570**	0.533**	0.515**
	(0.25)	(0.23)	(0.22)	(0.22)	(0.22)
W_dSPEI36-flo grw it-1	-0.250	-0.348	-0.683*	-0.679	-0.804*
	(0.37)	(0.39)	(0.40)	(0.42)	(0.42)
SPEI36-dro grw i,t-1	0.057	0.100	0.148	0.147	0.149
	(0.12)	(0.11)	(0.11)	(0.11)	(0.10)
W_dSPEI36-dro grw it-1	0.010	-0.067	-0.136	-0.118	-0.098
	(0.15)	(0.15)	(0.15)	(0.15)	(0.15)
Const	-4.046***	-2.758***	-1.508	-0.951	-0.052
	(0.94)	(1.00)	(1.05)	(1.10)	(1.18)
Fixed Effects (country)	Yes	Yes	Yes	Yes	Yes
Zero model					
No conflicts it-1	-2.597***	-2.587***	-2.579***	-2.581***	-2.567***
	(0.10)	(0.10)	(0.10)	(0.10)	(0.10)
Population i,t-1	-0.197***	-0.202***	-0.203***	-0.204***	-0.204***
	(0.04)	(0.03)	(0.03)	(0.03)	(0.03)
City (dummy) i	-0.137*	-0.126	-0.120	-0.121	-0.120
	(0.08)	(0.08)	(0.08)	(0.08)	(0.08)
Desert (dummy) i	0.194	0.208	0.215*	0.220*	0.224*
	(0.13)	(0.13)	(0.13)	(0.13)	(0.13)
Forested area (dummy) i	0.381***	0.399***	0.415***	0.426***	0.431***
	(0.13)	(0.13)	(0.13)	(0.13)	(0.13)
Const	4.272***	4.321***	4.316***	4.324***	4.311***
	(0.45)	(0.44)	(0.42)	(0.43)	(0.43)
Alpha	0.800***	0.789***	0.783***	0.783***	0.776***
	(0.04)	(0.04)	(0.04)	(0.04)	(0.04)
Observations	79590	79590	79590	79590	79590
Log-likelihood	-31316.454	-31272.926	-31230.817	-31219.868	-31195.731
Chi2	7792.088	4905.768	8037.807	6765.945	8455.841
AIC	62770.908	62683.851	62599.634	62577.737	62529.461
BIC	63411.548	63324.492	63240.275	63218.377	63170.102

Clustered (id) robust standard errors in parentheses. * $p < 0.1$, ** $p < 0.05$, *** $p < 0.01$.

Table A5: Alternative W_d matrix with ACLED (model 7)

	W_1	W_2	W_3	W_4	W_5
Count model					
Population i,t-1	0.457***	0.436***	0.437***	0.435***	0.436***
	(0.04)	(0.03)	(0.03)	(0.03)	(0.03)
W_dPopulation it-1	-0.063	-0.061	-0.072	-0.086**	-0.110**
	(0.04)	(0.04)	(0.04)	(0.04)	(0.04)
Change in GCPpc i,t-1	-1.054	-0.667	-0.501	-0.313	-0.348
	(1.18)	(1.08)	(1.03)	(0.98)	(0.90)
W_dChange in GCPpc it-1	-0.746	-1.299	-1.730	-2.108*	-2.252*
	(1.31)	(1.28)	(1.25)	(1.22)	(1.18)
Gini index i,t-1	1.022***	1.085***	1.054***	1.006***	0.951***
	(0.29)	(0.28)	(0.28)	(0.27)	(0.27)
W_dGini index it-1	-2.953***	-4.332***	-4.990***	-5.544***	-6.104***
	(0.47)	(0.58)	(0.70)	(0.75)	(0.84)
Ethnic fract i	0.141***	0.132***	0.131***	0.130***	0.134***
	(0.03)	(0.03)	(0.03)	(0.03)	(0.03)
Border cell (dummy) i	0.433***	0.430***	0.426***	0.425***	0.423***
	(0.08)	(0.08)	(0.08)	(0.08)	(0.08)
Long-term temp ch i,t-1	0.093	0.049	0.018	0.014	0.002
	(0.09)	(0.08)	(0.08)	(0.08)	(0.07)
W_dLong-term temp ch it-1	0.398***	0.491***	0.559***	0.579***	0.613***
	(0.09)	(0.09)	(0.09)	(0.09)	(0.09)
SPEI36-flo grw i,t-1	0.332*	0.213	0.226	0.195	0.151
	(0.19)	(0.17)	(0.18)	(0.17)	(0.17)
W_dSPEI36-flo grw it-1	1.395***	1.735***	1.801***	1.926***	2.118***
	(0.23)	(0.24)	(0.25)	(0.25)	(0.26)
SPEI36-dro grw i,t-1	0.039	0.055	0.086	0.083	0.085
	(0.08)	(0.08)	(0.08)	(0.08)	(0.08)
W_dSPEI36-dro grw it-1	0.036	0.025	-0.004	0.024	0.058
	(0.10)	(0.10)	(0.11)	(0.11)	(0.11)
Const	-5.368***	-4.470***	-3.945***	-3.394***	-2.715***
	(0.55)	(0.64)	(0.70)	(0.72)	(0.76)
Fixed Effects (country)	Yes	Yes	Yes	Yes	Yes
Zero model					
No conflicts it-1	-2.103***	-2.092***	-2.088***	-2.086***	-2.080***
	(0.10)	(0.10)	(0.10)	(0.10)	(0.10)
Population i,t-1	-0.266***	-0.273***	-0.272***	-0.275***	-0.276***
	(0.03)	(0.03)	(0.03)	(0.03)	(0.03)
City (dummy) i	-0.426***	-0.415***	-0.418***	-0.414***	-0.416***
	(0.07)	(0.07)	(0.07)	(0.07)	(0.07)
Desert (dummy) i	0.411***	0.362***	0.376***	0.365***	0.378***
	(0.12)	(0.12)	(0.11)	(0.12)	(0.12)
Forested area (dummy) i	0.450***	0.418***	0.430***	0.432***	0.435***
	(0.12)	(0.12)	(0.12)	(0.12)	(0.12)
Const	4.284***	4.374***	4.348***	4.377***	4.377***
	(0.35)	(0.35)	(0.35)	(0.35)	(0.35)
Alpha	0.671***	0.664***	0.664***	0.661***	0.660***
	(0.03)	(0.03)	(0.03)	(0.03)	(0.03)
Observations	61019	61019	61019	61019	61019
Log-likelihood	-40674.502	-40611.674	-40593.621	-40565.626	-40545.320
Chi2	2615.018	2396.800	2151.228	2049.417	2085.204
AIC	81487.003	81361.348	81325.242	81269.252	81228.641
BIC	82109.310	81983.655	81947.549	81891.559	81850.948

Clustered (id) robust standard errors in parentheses. * $p < 0.1$, ** $p < 0.05$, *** $p < 0.01$.

A.3 Robustness on econometric results

First, we run the following alternative specifications and robustness checks on our baseline specification for both UCDP (Table A6) and ACLED data (Table A7):

- We include the lagged number of conflict events in the count model rather than in the zero model (column 2);
- We employ the change in population rather than population in level (column 3);
- We replace GREG data on ethnic fractionalization with information from the Geo-referencing Ethnic Power Relations (Geo-EPR) dataset (column 4);
- We add a proxy for institutions at the country level (column 5);
- We replace the forest and desert dummy variables with the continuous information on the cell's area (%) covered by desert and forest (columns 6 and 7);
- We add the distance from the capital city among the covariates in the Count model (column 8).

In all cases results remain qualitatively unchanged, and our preferred specification (column 1) display the lowest value for AIC and BIC. The only two exceptions are the specifications reported in columns 5 and 8 (although the improvement in the AIC and BIC value is marginal). With respect to the country level of institutional quality (column 5), two additional reasons motivate our choice to not include this proxy in our model: i) given the nature of our forecasting exercise, we would require information about institutions also for future years (and possibly differentiated across SSPs), and we do not have such

information; ii) since our models include country fixed effects, country-level time-invariant characteristics like Colonial legacy are already accounted for. As for the distance from the capital city, we decide not to include it in our model since it may be problematic when it comes to the spatial models, as the value of this variable would be mechanically correlated across neighbouring cells.

Second, given that the socio-economic and climate variables for the period 2017-2020 are derived from SSPs scenarios, we also test potential divergences associated to the choice of the baseline scenario used. In Figures A14a-A14b we report the mean squared Pearson residuals per year obtained by running model 7 (including the indirect effects of climate variability through the agricultural channel mediated by the crops growing season) in Tables A1 and A2 with different values for the variables projected under the five SSPs for the validation period 2017-2020. Results from the five SSPs are quite similar, and we consider the SSP2 as the baseline up to 2020 and than we differentiate across SSPs for the forecasting exercise beyond 2020.

Third, robustness of statistical significance of coefficients in recursive windows for the validation period 2017-2020 for model 7 is provided in Tables A8-A9 for UCDP and ACLED, respectively (corresponding to a four-steps procedure of the recursive method application).

Fourth, robustness to alternative fixed effects specification is provided by Figure A15 where the mean Pearson residuals per year are plotted using country or cell fixed effects. Although residuals are lower in the case of cell fixed effects, the introduction of the term y_{it-1} in the *Zero model* combined with country fixed effects almost completely correct for

serial correlation, while avoiding potential biases deriving from an excess in number of fixed effects into non-linear models (Fernández-Val and Weidner, 2016).

Table A6: Baseline model selection 1990-2016 (UCDP conflicts)

	(1)	(2)	(3)	(4)	(5)	(6)	(7)	(8)
Count model								
No conflicts it-1		0.264***						
		(0.03)						
Population i,t-1	0.324***	0.365***		0.352***	0.319***	0.324***	0.323***	0.391***
	(0.07)	(0.04)		(0.07)	(0.07)	(0.07)	(0.07)	(0.10)
Change in GCPpc i,t-1	-2.571***	-3.007***	-2.587***	-2.547***	-2.931***	-2.568***	-2.567***	-2.679***
	(0.44)	(0.51)	(0.42)	(0.43)	(0.49)	(0.44)	(0.44)	(0.42)
Gini index i,t-1	0.394	0.685***	0.652	0.390	0.396	0.393	0.387	0.308
	(0.45)	(0.26)	(0.40)	(0.44)	(0.44)	(0.45)	(0.45)	(0.51)
Ethnic fract i	0.140***	0.074***	0.231***		0.137***	0.140***	0.140***	0.095**
	(0.04)	(0.03)	(0.04)		(0.04)	(0.04)	(0.04)	(0.04)
Border cell (dummy) i	0.301***	0.181***	0.324***	0.340***	0.299***	0.304***	0.301***	0.192*
	(0.10)	(0.07)	(0.11)	(0.11)	(0.10)	(0.10)	(0.10)	(0.10)
Change in population i, t-1			-7.528*					
			(4.10)					
ELF i, t				0.382***				
				(0.12)				
Governance c, t-1					3.303***			
					(0.84)			
Distance from capital city i								0.000***
								(0.00)
Const	-5.959***	-8.245***	-1.724***	-6.180***	-6.737***	-5.954***	-5.945***	-6.905***
	(0.87)	(0.48)	(0.41)	(0.85)	(0.88)	(0.87)	(0.87)	(1.21)
Zero model								
No conflicts it-1	-2.618***		-2.800***	-2.622***	-2.618***	-2.616***	-2.616***	-2.601***
	(0.10)		(0.11)	(0.10)	(0.10)	(0.10)	(0.10)	(0.10)
Population i,t-1	-0.180***	-0.091		-0.170***	-0.182***	-0.180***	-0.185***	-0.175***
	(0.04)	(0.06)		(0.04)	(0.04)	(0.04)	(0.04)	(0.05)
City (dummy) i	-0.152*	-0.173	-0.618***	-0.156*	-0.150*	-0.150*	-0.150*	-0.148*
	(0.08)	(0.50)	(0.08)	(0.08)	(0.08)	(0.08)	(0.08)	(0.09)
Desert (dummy) i	0.253**	13.196	1.141***	0.265**	0.291**	0.240*		0.331***
	(0.12)	(8.26)	(0.11)	(0.12)	(0.12)	(0.12)		(0.12)
Forest (dummy) i	0.395***	12.820	0.651***	0.388***	0.395***		0.385***	0.355***
	(0.13)	(8.13)	(0.13)	(0.13)	(0.13)		(0.13)	(0.13)
Change in population i, t-1			-22.153***					
			(3.40)					
Forest area i						0.321***		
						(0.11)		
Desert area i							0.207*	
							(0.11)	
Const	4.060***	-11.849	2.470***	3.939***	4.066***	4.073***	4.122***	3.962***
	(0.52)	(8.42)	(0.10)	(0.51)	(0.51)	(0.52)	(0.51)	(0.62)
Alpha	0.852***	1.986***	0.920***	0.851***	0.848***	0.851***	0.851***	0.838***
	(0.04)	(0.05)	(0.05)	(0.04)	(0.04)	(0.04)	(0.04)	(0.04)
Observations	79590	79590	79590	79590	79590	79590	79590	79590
Log-likelihood	-31494.001	-33059.094	-32031.298	-31504.038	-31470.559	-31495.433	-31495.142	-31406.568
Chi2	8165.713	15829.150	10175.984	7299.763	7470.721	8150.725	8097.161	14168.000
AIC	63108.002	66238.188	64182.596	63128.077	63063.119	63110.867	63110.284	62935.135
BIC	63665.080	66795.266	64739.674	63685.155	63629.482	63667.945	63667.363	63501.499

Standard errors in parentheses
* $p < 0.1$, ** $p < 0.05$, *** $p < 0.01$

Table A7: Baseline model selection 1990-2016 (ACLED conflicts)

	(1)	(2)	(3)	(4)	(5)	(6)	(7)	(8)
Count model								
No conflicts it-1		0.120***						
		(0.02)						
Population i,t-1	0.474***	0.430***		0.500***	0.467***	0.474***	0.474***	0.577***
	(0.03)	(0.03)		(0.03)	(0.03)	(0.03)	(0.03)	(0.03)
Change in GCPpc i,t-1	-1.344***	-1.581***	-1.275***	-1.387***	-1.797***	-1.340***	-1.344***	-1.530***
	(0.24)	(0.32)	(0.22)	(0.23)	(0.24)	(0.24)	(0.24)	(0.22)
Gini index i,t-1	0.748***	0.765***	1.481***	0.706**	0.762***	0.746***	0.743***	0.600**
	(0.28)	(0.19)	(0.33)	(0.29)	(0.28)	(0.28)	(0.28)	(0.28)
Ethnic fract i	0.158***	0.078***	0.260***		0.159***	0.159***	0.158***	0.121***
	(0.03)	(0.02)	(0.04)		(0.03)	(0.03)	(0.03)	(0.03)
Border cell (dummy) i	0.473***	0.341***	0.403***	0.520***	0.470***	0.476***	0.473***	0.328***
	(0.08)	(0.06)	(0.09)	(0.08)	(0.08)	(0.08)	(0.08)	(0.07)
Change in population i, t-1			-2.598					
			(2.46)					
ELF i, t				0.404***				
				(0.10)				
Governance c, t-1					4.955***			
					(0.74)			
Distance from capital city i								0.000***
								(0.00)
Const	-7.071***	-7.148***	-1.223***	-7.231***	-8.212***	-7.071***	-7.076***	-8.494***
	(0.48)	(0.43)	(0.31)	(0.49)	(0.50)	(0.48)	(0.48)	(0.49)
Zero model								
No conflicts it-1	-2.094***		-2.386***	-2.098***	-2.097***	-2.096***	-2.093***	-2.100***
	(0.09)		(0.11)	(0.09)	(0.10)	(0.09)	(0.09)	(0.10)
Population i,t-1	-0.263***	-0.417***		-0.254***	-0.269***	-0.264***	-0.266***	-0.246***
	(0.03)	(0.07)		(0.03)	(0.03)	(0.03)	(0.03)	(0.03)
City (dummy) i	-0.414***	-5.756***	-1.201***	-0.424***	-0.409***	-0.413***	-0.415***	-0.419***
	(0.07)	(1.78)	(0.07)	(0.07)	(0.07)	(0.07)	(0.07)	(0.07)
Desert (dummy) i	0.408***	1.031***	1.685***	0.413***	0.450***	0.390***		0.514***
	(0.11)	(0.34)	(0.09)	(0.11)	(0.11)	(0.11)		(0.11)
Forest (dummy) i	0.454***	1.678***	0.747***	0.459***	0.424***		0.446***	0.298**
	(0.12)	(0.30)	(0.13)	(0.12)	(0.12)		(0.12)	(0.12)
Change in population i, t-1			-14.402***					
			(4.58)					
Forest area i						0.340***		
						(0.10)		
Desert area i							0.370***	
							(0.10)	
Const	4.323***	3.507***	1.634***	4.215***	4.380***	4.348***	4.370***	4.053***
	(0.36)	(0.91)	(0.11)	(0.37)	(0.36)	(0.36)	(0.35)	(0.36)
Alpha	0.722***	1.199***	0.854***	0.730***	0.712***	0.722***	0.720***	0.707***
	(0.04)	(0.06)	(0.04)	(0.04)	(0.04)	(0.04)	(0.04)	(0.04)
Observations	61019	61019	61019	61019	61019	61019	61019	61019
Log-likelihood	-41308.969	-42020.602	-42729.232	-41336.630	-41242.763	-41312.786	-41308.993	-41085.085
Chi2	1568.011	2049.889	1495.702	1616.227	1600.975	1569.610	1562.395	1659.894
AIC	82737.939	84161.204	85578.464	82793.260	82607.527	82745.572	82737.986	82292.169
BIC	83279.075	84702.340	86119.600	83334.397	83157.682	83286.709	83279.122	82842.324

Standard errors in parentheses
* $p < 0.1$, ** $p < 0.05$, *** $p < 0.01$

Table A8: Robustness with recursive forecast on model (7) Table A1 (2017-2020)

	(1) 2017	(2) 2018	(3) 2019	(4) 2020
Count model				
Population i,t-1	0.313***	0.296***	0.296***	0.293***
	(0.07)	(0.07)	(0.06)	(0.06)
Change in GCPpc i,t-1	-2.957***	-3.353***	-3.428***	-3.460***
	(0.50)	(0.61)	(0.60)	(0.58)
Gini index i,t-1	0.528	0.501	0.467	0.443
	(0.43)	(0.43)	(0.40)	(0.37)
Ethnic fract i	0.074*	0.092**	0.094***	0.094***
	(0.04)	(0.04)	(0.03)	(0.03)
Border cell (dummy) i	0.240**	0.249***	0.249***	0.245***
	(0.10)	(0.10)	(0.09)	(0.08)
Long-term temp ch i,t-1	0.585***	0.293***	0.236***	0.203***
	(0.12)	(0.07)	(0.04)	(0.03)
SPEI36-flo grw i,t-1	0.839***	0.542***	0.526***	0.522***
	(0.20)	(0.19)	(0.18)	(0.17)
SPEI36-dro grw i,t-1	0.080	0.091	0.112	0.118*
	(0.09)	(0.08)	(0.07)	(0.07)
Const	-6.323***	-6.135***	-6.065***	-5.911***
	(0.84)	(0.83)	(0.80)	(0.76)
Zero model				
No conflicts it-1	-2.594***	-2.806***	-3.616***	-3.330***
	(0.12)	(0.14)	(0.19)	(0.13)
Population i,t-1	-0.174***	-0.254***	-0.264***	-0.265***
	(0.04)	(0.04)	(0.04)	(0.03)
City (dummy) i	-0.184**	-0.112	-0.105	-0.097
	(0.09)	(0.08)	(0.08)	(0.07)
Desert (dummy) i	0.392***	0.271**	0.243**	0.222**
	(0.13)	(0.11)	(0.11)	(0.10)
Forest (dummy) i	0.369***	0.488***	0.505***	0.513***
	(0.14)	(0.13)	(0.13)	(0.12)
Const	3.960***	4.696***	4.914***	5.041***
	(0.51)	(0.49)	(0.47)	(0.44)
Alpha	0.816***	0.813***	0.647***	0.423***
	(0.04)	(0.04)	(0.04)	(0.04)
Observations	68978	71631	74284	76937
Log-likelihood	-25048.747	-27897.364	-30257.809	-32577.158
Chi2	7361.984	6483.437	7446.110	8729.612
AIC	50223.494	55920.728	60641.618	65280.317
BIC	50799.411	56499.022	61222.204	65863.114

Clustered (id) robust standard errors in parentheses. * $p < 0.1$, ** $p < 0.05$, *** $p < 0.01$.

Table A9: Robustness with recursive forecast on model (7) Table A2 (2017-2020)

	(1) 2017	(2) 2018	(3) 2019	(4) 2020
Count model				
Population i,t-1	0.454***	0.469***	0.473***	0.469***
	(0.03)	(0.03)	(0.03)	(0.03)
Change in GCPpc i,t-1	-2.032***	-2.156***	-2.165***	-2.161***
	(0.22)	(0.24)	(0.24)	(0.24)
Gini index i,t-1	1.034***	1.021***	0.990***	0.970***
	(0.30)	(0.29)	(0.27)	(0.26)
Ethnic fract i	0.109***	0.118***	0.122***	0.125***
	(0.03)	(0.03)	(0.03)	(0.02)
Border cell (dummy) i	0.383***	0.391***	0.388***	0.386***
	(0.08)	(0.08)	(0.07)	(0.06)
Long-term temp ch i,t-1	0.493***	0.336***	0.288***	0.256***
	(0.10)	(0.06)	(0.04)	(0.03)
SPEI36-flo grw i,t-1	1.159***	1.003***	0.950***	0.907***
	(0.14)	(0.12)	(0.11)	(0.11)
SPEI36-dro grw i,t-1	0.170**	0.179**	0.196***	0.206***
	(0.08)	(0.07)	(0.06)	(0.06)
Const	-7.340***	-7.530***	-7.539***	-7.430***
	(0.50)	(0.48)	(0.45)	(0.43)
Zero model				
No conflicts it-1	-2.023***	-2.225***	-2.903***	-2.915***
	(0.11)	(0.13)	(0.18)	(0.16)
Population i,t-1	-0.299***	-0.335***	-0.339***	-0.342***
	(0.03)	(0.03)	(0.03)	(0.03)
City (dummy) i	-0.407***	-0.333***	-0.308***	-0.296***
	(0.08)	(0.08)	(0.07)	(0.07)
Desert (dummy) i	0.589***	0.521***	0.500***	0.467***
	(0.12)	(0.11)	(0.11)	(0.10)
Forest (dummy) i	0.448***	0.437***	0.424***	0.407***
	(0.13)	(0.12)	(0.12)	(0.11)
Const	4.668***	4.967***	5.113***	5.270***
	(0.41)	(0.40)	(0.38)	(0.36)
Alpha	0.739***	0.638***	0.471***	0.279***
	(0.04)	(0.04)	(0.04)	(0.05)
Observations	50407	53060	55713	58366
Log-likelihood	-28683.570	-31896.713	-34766.629	-37650.026
Chi2	1554.275	1842.469	2183.143	2592.825
AIC	57493.141	63919.426	69659.258	75426.052
BIC	58049.298	64478.814	70221.720	75991.445

Clustered (id) robust standard errors in parentheses. * $p < 0.1$, ** $p < 0.05$, *** $p < 0.01$.

Figure A14: Model comparison on mean squared Pearson residuals (UCDP and ACLED)

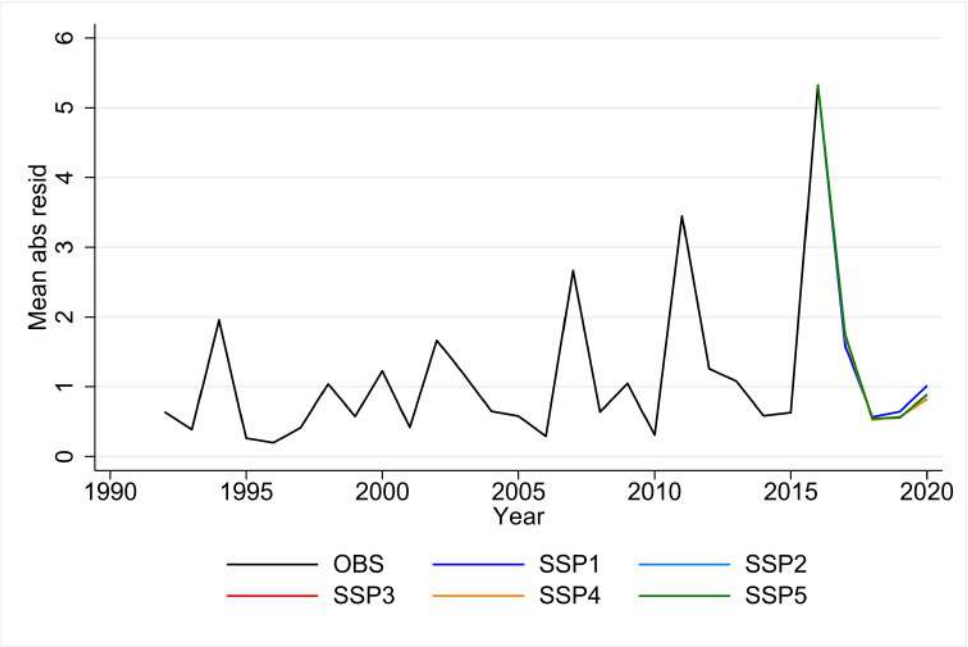

(a) Baseline validation UCDP (2017-2020)

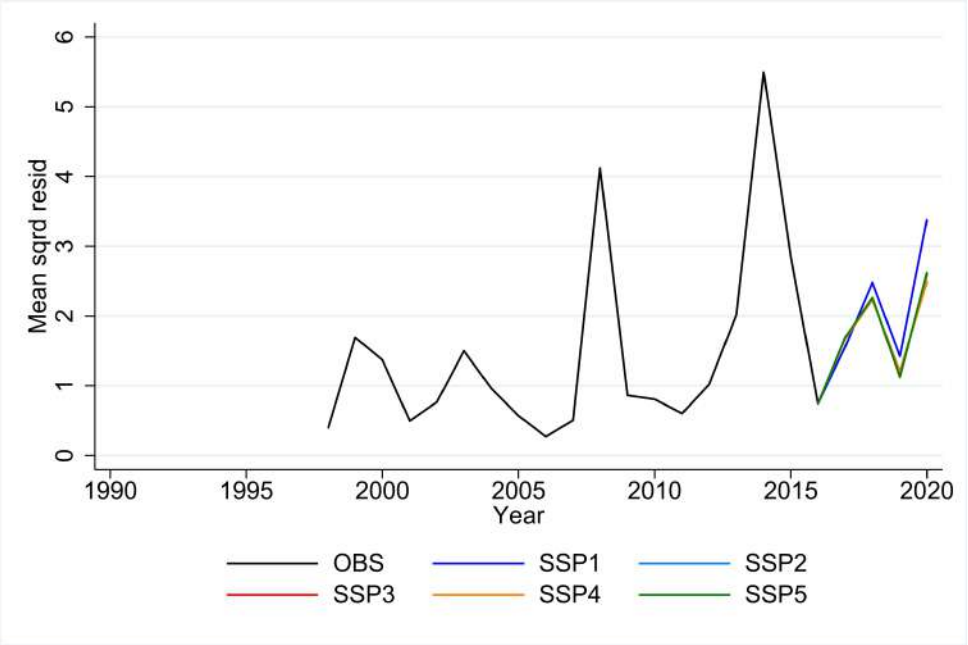

(b) Baseline validation ACLED (2017-2020)

Figure A15: Pearson residuals with country (CE) and cell (FE) fixed effects

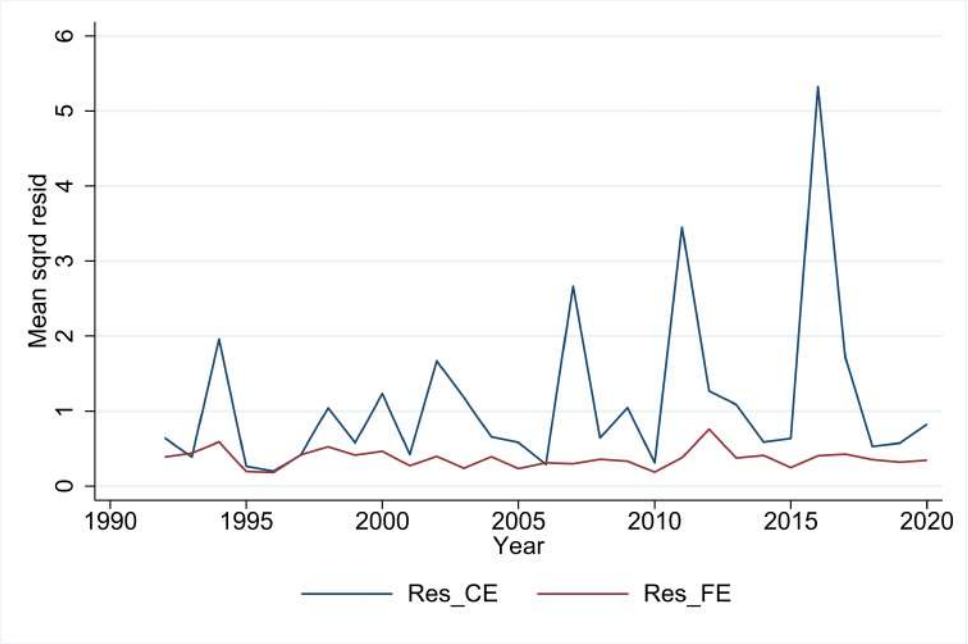

(a) Model (7) in Table A1 with UCDP

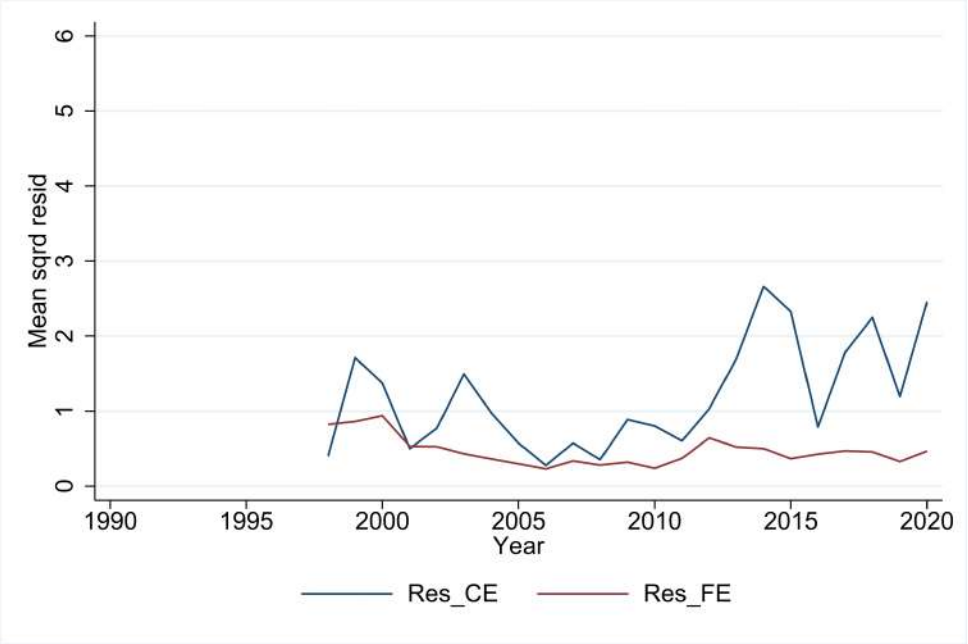

(b) Model (7) in Table A2 with ACLED

References

Basedau, M. and Pierskalla, J. H. (2014). How ethnicity conditions the effect of oil and gas on civil conflict: A spatial analysis of Africa from 1990 to 2010. *Political Geography*, 38:1–11.

Bosetti, V., Cattaneo, C., and Peri, G. (2021). Should they stay or should they go? Climate migrants and local conflicts. *Journal of Economic Geography*, 21(4):619–651.

Buhaug, H. and Urdal, H. (2013). An urbanization bomb? Population growth and social disorder in cities. *Global Environmental Change*, 23(1):1–10.

Burke, M., Hsiang, S. M., and Miguel, E. (2015). Climate and Conflict. *Annual Review of Economics*, 7(1):577–617.

Chassang, S. and i Miquel, G. P. (2009). Economic shocks and civil war. *Quarterly Journal of Political Science*, 4(3):211–228.

Corrales, L. M. G., Avila, H., and Gutierrez, R. R. (2019). Land-use and socioeconomic changes related to armed conflicts: A Colombian regional case study. *Environmental Science & Policy*, 97:116–124.

Crespo Cuaresma, J. (2017). Income projections for climate change research: A framework based on human capital dynamics. *Global Environmental Change*, 42:226–236.

De Stefano, L., Petersen-Perlman, J. D., Sproles, E. A., Eynard, J., and Wolf, A. T. (2017). Assessment of transboundary river basins for potential hydro-political tensions. *Global Environmental Change*, 45:35–46.

Fernández-Val, I. and Weidner, M. (2016). Individual and time effects in nonlinear panel models with large N, T. *Journal of Econometrics*, 192(1):291–312.

Gleditsch, N. P., Wallensteen, P., Eriksson, M., Strand, H., Sarkees, M. R., and Smith, D. (2002). Armed Conflict 1946 – 2001 : A New Dataset *. 39(5):615–637.

Goldewijk, K. K., Beusen, A., Doelman, J., and Stehfest, E. (2017). Anthropogenic land use estimates for the Holocene - HYDE 3.2. *Earth System Science Data*, 9(2):927–953.

Hayes, M., Svoboda, M., Wall, N., and Widhalm, M. (2011). The lincoln declaration on drought indices: Universal meteorological drought index recommended. *Bulletin of the American Meteorological Society*, 92(4):485–488.

Hsiang, S. M., Meng, K. C., and Cane, M. A. (2011). Civil conflicts are associated with the global climate. *Nature*, 476(7361):438–441.

Ide, T., Schilling, J., Link, J. S., Scheffran, J., Ngaruiya, G., and Weinzierl, T. (2014). On exposure, vulnerability and violence: Spatial distribution of risk factors for climate change and violent conflict across Kenya and Uganda. *Political Geography*, 43:68–81.

Jones, B. and O'Neill, B. C. (2016). Spatially explicit global population scenarios consistent with the Shared Socioeconomic Pathways. *Environmental Research Letters*, 11(8).

Jones, B. T., Mattiacci, E., and Braumoeller, B. F. (2017). Food scarcity and state vulnerability: Unpacking the link between climate variability and violent unrest. *Journal of Peace Research*, 54(3):335–350.

Kummu, M., Taka, M., and Guillaume, J. H. (2018). Gridded global datasets for Gross Domestic Product and Human Development Index over 1990-2015. *Scientific Data*, 5:1–15.

La Ferrara, E. and Harari, M. (2018). Conflict, climate and cells: A disaggregated analysis. *Review of Economics and Statistics*, 100(4):594–608.

McKee, T. B., Doesken, N. J., and Kleist, J. (1993). The relationship of drought frequency and duration to time scales. 17(22):179–183.

O'Loughlin, J., Linke, A. M., and Witmer, F. D. (2014). Effects of temperature and precipitation variability on the risk of violence in sub-saharan africa, 1980–2012. *Proceedings of the National Academy of Sciences*, 111(47):16712–16717.

O'Loughlin, J., Witmer, F. D., Linke, A. M., Laing, A., Gettelman, A., and Dudhia, J. (2012). Climate variability and conflict risk in east africa, 1990–2009. *Proceedings of the National Academy of Sciences*, 109(45):18344–18349.

Pandey, R. P. and Ramasastri, K. S. (2001). Relationship between the common climatic parameters and average drought frequency. *Hydrological Processes*, 15(6):1019–1032.

Papaioannou, K. J. (2016). Climate shocks and conflict: Evidence from colonial Nigeria. *Political Geography*, 50:33–47.

Parsons, D. J., Rey, D., Tanguy, M., and Holman, I. P. (2019). Regional variations in the link between drought indices and reported agricultural impacts of drought. *Agricultural Systems*, 173(September 2018):119–129.

Riahi, K., van Vuuren, D. P., Kriegler, E., Edmonds, J., O'Neill, B. C., Fujimori, S., Bauer, N., Calvin, K., Dellink, R., Fricko, O., Lutz, W., Popp, A., Cuaresma, J. C., KC, S., Leimbach, M., Jiang, L., Kram, T., Rao, S., Emmerling, J., Ebi, K., Hasegawa, T., Havlik, P., Humpenöder, F., Da Silva, L. A., Smith, S., Stehfest, E., Bosetti, V., Eom, J., Gernaat, D., Masui, T., Rogelj, J., Strefler, J., Drouet, L., Krey, V., Luderer, G., Harmsen, M., Takahashi, K., Baumstark, L., Doelman, J. C., Kainuma, M., Klimont, Z., Marangoni, G., Lotze-Campen, H., Obersteiner, M., Tabeau, A., and Tavoni, M. (2017). The Shared Socioeconomic Pathways and their energy, land use, and greenhouse gas emissions implications: An overview. *Global Environmental Change*, 42:153–168.

Samir, K. C. and Lutz, W. (2017). The human core of the shared socioeconomic pathways: Population scenarios by age, sex and level of education for all countries to 2100. *Global Environmental Change*, 42:181–192.

Schleussner, C.-F., Donges, J. F., Donner, R. V., and Schellnhuber, H. J. (2016). Armed-conflict risks enhanced by climate-related disasters in ethnically fractionalized countries. *Proceedings of the National Academy of Sciences*, 113(33):9216–9221.

Sheffield, J., Wood, E. F., Chaney, N., Guan, K., Sadri, S., Yuan, X., Olang, L., Amani, A., Ali, A., Demuth, S., et al. (2014). A drought monitoring and forecasting system for sub-sahara african water resources and food security. *Bulletin of the American Meteorological Society*, 95(6):861–882.

Vicente-Serrano, S. M., Beguería, S., and López-Moreno, J. I. (2010). A multiscalar drought index sensitive to global warming: The standardized precipitation evapotranspiration index. *Journal of Climate*, 23(7):1696–1718.

Von Uexkull, N., Croicu, M., Fjelde, H., and Buhaug, H. (2016). Civil conflict sensitivity to growing-season drought. *Proceedings of the National Academy of Sciences of the United States of America*, 113(44):12391–12396.

Weidmann, N. B., Rød, J. K., and Cederman, L.-E. (2010). Representing ethnic groups in space: A new dataset. *Journal of Peace Research*, 47(4):491–499.

Yang, W., Andréasson, J., Graham, L. P., Olsson, J., Rosberg, J., and Wetterhall, F. (2010). Distribution-based scaling to improve usability of regional climate model projections for hydrological climate change impacts studies. *Hydrology Research*, 41(3-4):211–229.